© 2015. Published by The Company of Biologists Ltd | Journal of Cell Science (2015) 128, 4462 doi:10.1242/jcs.182360

CORRECTION

Sonic hedgehog processing and release are regulated by glypican heparan sulfate proteoglycans

Corinna Ortmann, Ute Pickhinke, Sebastian Exner, Stefanie Ohlig, Roger Lawrence, Hamodah Jboor, Rita Dreier and Kay Grobe

There was an error published in *J. Cell Sci.* **128**, 2374-2385.

The reference Oustah et al. (2014) was cited incorrectly throughout the manuscript and in the reference list. Citations of Oustah et al. (2014) should read Al Oustah et al. (2014), and the correct reference is given below.

Al Oustah, A., Danesin, C., Khouri-Farah, N., Farreny, M.-A., Escalas, N., Cochard, P., Glise, B. and Soula, C. (2014). Dynamics of Sonic hedgehog signaling in the ventral spinal cord are controlled by intrinsic changes in source cells requiring Sulfatase 1. *Development* **141**, 1392-1403.

Journal of Cell Science and the authors apologise to the readers for any confusion that this error might have caused.

Journal of Cell Science

© 2015. Published by The Company of Biologists Ltd | Journal of Cell Science (2015) 128, 2374-2385 doi:10.1242/jcs.170670

RESEARCH ARTICLE

Sonic hedgehog processing and release are regulated by glypican heparan sulfate proteoglycans

Corinna Ortmann[1], Ute Pickhinke[1], Sebastian Exner[1], Stefanie Ohlig[1], Roger Lawrence[2], Hamodah Jboor[1], Rita Dreier[1,3] and Kay Grobe[1,3,*]

ABSTRACT

All Hedgehog morphogens are released from producing cells, despite being synthesized as N- and C-terminally lipidated molecules, a modification that firmly tethers them to the cell membrane. We have previously shown that proteolytic removal of both lipidated peptides, called shedding, releases bioactive Sonic hedgehog (Shh) morphogens from the surface of transfected Bosc23 cells. Using *in vivo* knockdown together with *in vitro* cell culture studies, we now show that glypican heparan sulfate proteoglycans regulate this process, through their heparan sulfate chains, in a cell autonomous manner. Heparan sulfate specifically modifies Shh processing at the cell surface, and purified glycosaminoglycans enhance the proteolytic removal of N- and C-terminal Shh peptides under cell-free conditions. The most likely explanation for these observations is direct Shh processing in the extracellular compartment, suggesting that heparan sulfate acts as a scaffold or activator for Shh ligands and the factors required for their turnover. We also show that purified heparan sulfate isolated from specific cell types and tissues mediates the release of bioactive Shh from pancreatic cancer cells, revealing a previously unknown regulatory role for these versatile molecules in a pathological context.

KEY WORDS: Glycosaminoglycan, Sonic hedgehog, Shedding, Glypican, Heparan sulfate

INTRODUCTION

A major challenge in developmental biology is to understand how cells coordinate their developmental behavior with that of their neighbors. Cells often use signaling molecules from a local source that act at a distance on target cells. The proteins of the Hedgehog (Hh) family are one such group of signaling molecules that control development and contribute to cancer formation and progression in the adult (Theunissen and de Sauvage, 2009; Yauch et al., 2008). Vertebrates produce three structurally and functionally related Hh proteins [Sonic Hh (Shh), Indian Hh (Ihh) and Desert Hh]. Production of the active 19-kDa Shh protein begins with covalent attachment of a cholesterol moiety to the carbonyl moiety of its C-terminal glycine residue. In a second step, Hh acyltransferase (Hhat) attaches a palmitoyl group to the NH_2-terminal cysteine of the Shh signaling domain. The dually lipidated molecule constitutes the active morphogen (Jacob and Lum, 2007). Upon secretion to the cell surface, lipidated Hh proteins multimerize and then transport to cells expressing the Hh receptor Patched (Panáková et al., 2005; Zeng et al., 2001). The paradox is that these membrane-tethered Hh molecules serve as long-range morphogens, suggesting that specific mechanisms are required for their release and transport.

One group of molecules involved in Shh solubilization are a disintegrin and metalloproteinase (ADAM) sheddases (Dierker et al., 2009; Ohlig et al., 2011). Sheddases release numerous membrane-associated molecules from the cell surface (summarized in Tellier et al., 2006; Yang et al., 2006), while the cell retains the membrane-associated remnant peptides. However, because redundancy in enzymes and substrates is common (Kheradmand and Werb, 2002), activities and colocalization of sheddases with their substrate(s) requires tight regulation. One recently described Hh shedding regulator is the glycoprotein Scube2 (signal peptide, cubulin domain, epidermal growth factor-like protein 2) (Jakobs et al., 2014). Another group of molecules that regulate Hh signaling is the glycosylphosphatidylinositol (GPI)-linked glypican (Gpc) heparan sulfate proteoglycans (HSPGs, Gpc1–Gpc6 in vertebrates) (Chatterjee and Mayor, 2001; Mayor and Riezman, 2004; Rietveld et al., 1999), called Division abnormally delayed (Dally) (Nakato et al., 1995) and Dally-like protein (Dlp) (Khare and Baumgartner, 2000) in the fly. Gpc functions often depend on their heparan sulfate glycosaminoglycan chains, which are produced by virtually all cells as part of the cell surface and extracellular matrix (Esko and Lindahl, 2001). The unbranched heparan sulfate chain is synthesized by glycosyltransferases Ext1 and Ext2, or by the Tout-velu (Ttv) and Sister of tout velu orthologs in *Drosophila*. The nascent heparan sulfate chain consists of repeating glucuronic acid and N-acetylglucosamine $(GlcA\beta1,4GlcNAc\alpha1,4)_n$ disaccharide units that undergo modification by one or more of the four N-deacetylase/N-sulfotransferase isozymes [or the single Sulfateless (Sfl) ortholog in the fly (Toyoda et al., 2000)]. The resulting N-sulfoglucosamine (GlcNS)-containing chain is further modified by one 2-O-sulfotransferase, several 3-O- and 6-O-sulfotransferases, and a GlcA C5-epimerase, the latter converting GlcA into iduronic acid (IduA) (Esko and Selleck, 2002; Lindahl et al., 1998). Finally, heparan sulfate sulfation in the extracellular compartment is reduced by the secreted 6-O-endosulfatase 1 (Sulf1) and its homolog Sulf2 in vertebrates, or by the Sulf1 fly ortholog (Lamanna et al., 2006). Together, these activities result in vertebrate heparan sulfate consisting of multiple unmodified NAc (N-acetylated), highly sulfated N-sulfated, and mixed NAc and N-sulfated domains (Carlsson et al., 2008). In *Drosophila*, heparan sulfate consists of a single extended N-sulfated domain (Kusche-Gullberg et al., 2012). Heparin represents a highly sulfated form of heparan sulfate, mostly consisting of disulfated (26%) and trisulfated (73%) disaccharides and a minor monosulfated or non-sulfated fraction containing GlcA or IduA linked to GlcNAc and GlcNS (1%) (Saad et al., 2005). Heparan sulfate and heparin binding of various

[1]Institute for Physiological Chemistry and Pathobiochemistry, University of Münster, 48149 Münster, Germany. [2]Department of Cellular and Molecular Medicine, University of California San Diego, La Jolla, CA 92093, USA. [3]Cells-in-Motion Cluster of Excellence (EXC1003-CiM), University of Münster, 48149 Münster, Germany.

*Author for correspondence (kgrobe@uni-muenster.de)

Received 24 February 2015; Accepted 5 May 2015

Journal of Cell Science

Journal of Cell Science (2015) 128, 2374-2385 doi:10.1242/jcs.170670

morphogens, cytokines, chemokines, growth factors, proteases and protease inhibitors is mediated by clusters of basic amino acids on their surfaces. In vertebrate Hh proteins, heparan sulfate is mainly bound by the Cardin–Weintraub motif BBBxxBB (B represents a basic amino acid, x represents any amino acid) (Cardin and Weintraub, 1989; Chang et al., 2011; Farshi et al., 2011; Rubin et al., 2002), but Cardin–Weintraub residues also constitute the N-terminal Hh sheddase cleavage site (Ohlig et al., 2012). This suggests a possible mode of processing regulation by competitive heparan sulfate binding, consistent with recently described HSPG bioactivities in Hh-producing cells (Ayers et al., 2010; Bilioni et al., 2013; Oustah et al., 2014; Wojcinski et al., 2011). In the present study, we provide evidence that supports this functional link. We found that Gpc HSPGs regulate Shh release from producing cells *in vitro* and *in vivo* and that heparan sulfate regulates proteolytic Shh processing *in vitro*. We further show that purified heparan sulfate directly stimulates Shh processing and that this ability depends on the source of heparan sulfate. This finding indicates that there are heparan-sulfate-dependent Hh ligand or release factor scaffolding or activator functions in the extracellular compartment. It further reveals a previously unknown role of cell surface HSPGs in the precise control of spatiotemporal Hh signaling.

RESULTS

Loss of Dally function in Hh-producing cells affects *Drosophila* wing patterning

Embryonic null mutants for the genes *dally* and *dlp* (Ayers et al., 2010; Gallet et al., 2008; Han et al., 2004b; Takeo et al., 2005; Williams et al., 2010) and mutants for heparan sulfate biosynthetic genes *ttv* (Bellaiche et al., 1998; The et al., 1999), *brother of ttv* and *sister of ttv* (Bornemann et al., 2004; Han et al., 2004a; Takei et al., 2004) have phenotypes similar to *hh*-null mutants. These defects have been attributed to impaired Hh transport and reception. Moreover, it was recently reported that overexpression of the heparan-sulfate-modifying extracellular enzyme *Drosophila* sulfatase (Sulf1) in Hh-producing posterior wing disc cells increased Hh patterning activity *in vivo* and that *sulf1* knockdown in these cells impaired Hh function (Wojcinski et al., 2011). This finding implied that the heparan sulfate expressed in Hh-producing cells can also regulate Hh biofunction (Oustah et al., 2014; Wilson and Chuang, 2006). To confirm this function, we downregulated HSPG expression *in vivo*, using Hh-dependent *Drosophila* wing development as a read-out. In the fly, wing development is initiated by Hh expression in the posterior wing disc compartment in response to the Engrailed (En) transcription factor (summarized in Crozatier et al., 2004; Hartl and Scott, 2014). Hh proteins are then released from posterior cells to move anteriorly. The position of the longitudinal L3–L4 wing veins results from this anterior Hh movement and can therefore be used to quantify the positional information provided by Hh, i.e. reduced Hh biofunction reduces the L3–L4 intervein region and concomitantly increases the L2–L3 intervein space (Crozatier et al., 2004; Lee et al., 2001; Mullor et al., 1997; Strigini and Cohen, 1997) (schematic in Fig. 1). We used the en-Gal4/UAS system to express various RNA interference (RNAi) constructs to target heparan sulfate biosynthetic enzymes or HSPG core proteins in Hh-producing posterior cells *in vivo*. Initial knockdown of the heparan sulfate biosynthetic genes *sfl* and *ttv* led to strong pleiotropic defects, lack of wings, or larval or pupal lethality that prevented further analysis (data not shown). *Drosophila* that were partially deficient in *dally* and *dlp* expression, however, survived and showed significantly impaired Hh-dependent wing patterning. A quantitative wing analysis revealed that the ratio between the L3–L4 and L2–L3

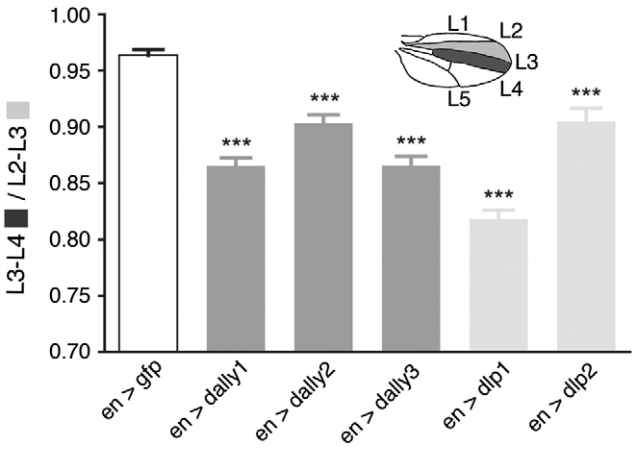

Fig. 1. Impaired HSPG expression in the posterior-compartment cells of the *Drosophila* wing affects Hh-dependent patterning *in vivo*. Inset, schematic of a *Drosophila melanogaster* wing. The area defined by the L3–L4 veins (dark gray) was quantified and the values obtained were divided by the L2–L3 area (light gray). This served as a read-out of Hh patterning activity (Crozatier et al., 2004). Graph, ratios between the L3–L4 and L2–L3 wing areas. Three different UAS-*dally* RNAi strains (dally1–dally3) were used, two UAS-*dlp* RNAi strains (dlp1, dlp2), and one UAS-*gfp*-RNAi control strain (gfp). ***P<0.0001 (two-tailed Student's t-test).

intervein areas decreased from 0.96±0.005 [en>GFP RNAi control (n=42)] to 0.86±0.007 (en>dally1, −10.23%), 0.9±0.007 (en>dally2, −6.27%), and 0.86±0.008 (en>dally3, −10.2%) (all mean±s.d., n=20, Fig. 1). This result demonstrates that impaired *dally* expression in all three independent RNAi fly lines (dally1–dally3) affected Hh function. Two independent RNAi lines targeting *dlp* expression also displayed reduced Hh function (en>dlp1, 0.82±0.008, −15.1% and en>dlp2, 0.9±0.012, −6.13%). Thus, both *Drosophila* glypicans have overlapping functions in Hh-producing cells. Because these observed phenotypes strongly resemble wing patterning defects seen upon RNAi-mediated *sulf1* knockdown (Wojcinski et al., 2011), we hypothesized that heparan sulfate modulates Hh multimerization prior to its release (Vyas et al., 2008) or impairs Hh release from the cell surface.

Cell-surface heparan sulfate regulates Shh processing *in vitro*

All Hh proteins are dual-lipidated proteins that firmly tether to the membrane of the cell that produces them. C-terminal Hh lipidation uses a strictly coupled cleavage and cholesterol esterification reaction (Bumcrot et al., 1995; Lee et al., 1994; Liu, 2000; Tabata and Kornberg, 1994) to render all 19-kDa Hh signaling domains insoluble (Liu, 2000; Marti et al., 1995; Porter et al., 1996a,b). The second Hh lipid modification is palmitic acid attached by Hhat to conserved N-terminal Hh cysteine residues (Amanai and Jiang, 2001; Chamoun et al., 2001; Lee and Treisman, 2001; Micchelli et al., 2002; Pepinsky et al., 1998) (Fig. 2A). We and others have shown that proteolytic removal of N- and C-terminal lipidated peptides (called shedding) releases bioactive Shh morphogens from the surface of producing cells *in vitro* (Damhofer et al., 2015; Dierker et al., 2009; Jakobs et al., 2014; Ohlig et al., 2011). We further showed that because of the lack of the N-terminal Hhat acceptor cysteine (C25S or C25A in mouse Shh) (Hardy and Resh, 2012) non-palmitoylated Hh proteins require only C-terminal shedding for their solubilization, whereas most Shh N-termini are left intact (Jakobs et al., 2014). Here, we confirm this observation by SDS-PAGE and immunoblotting of N-palmitoylated Shh and

Journal of Cell Science (2015) 128, 2374-2385 doi:10.1242/jcs.170670

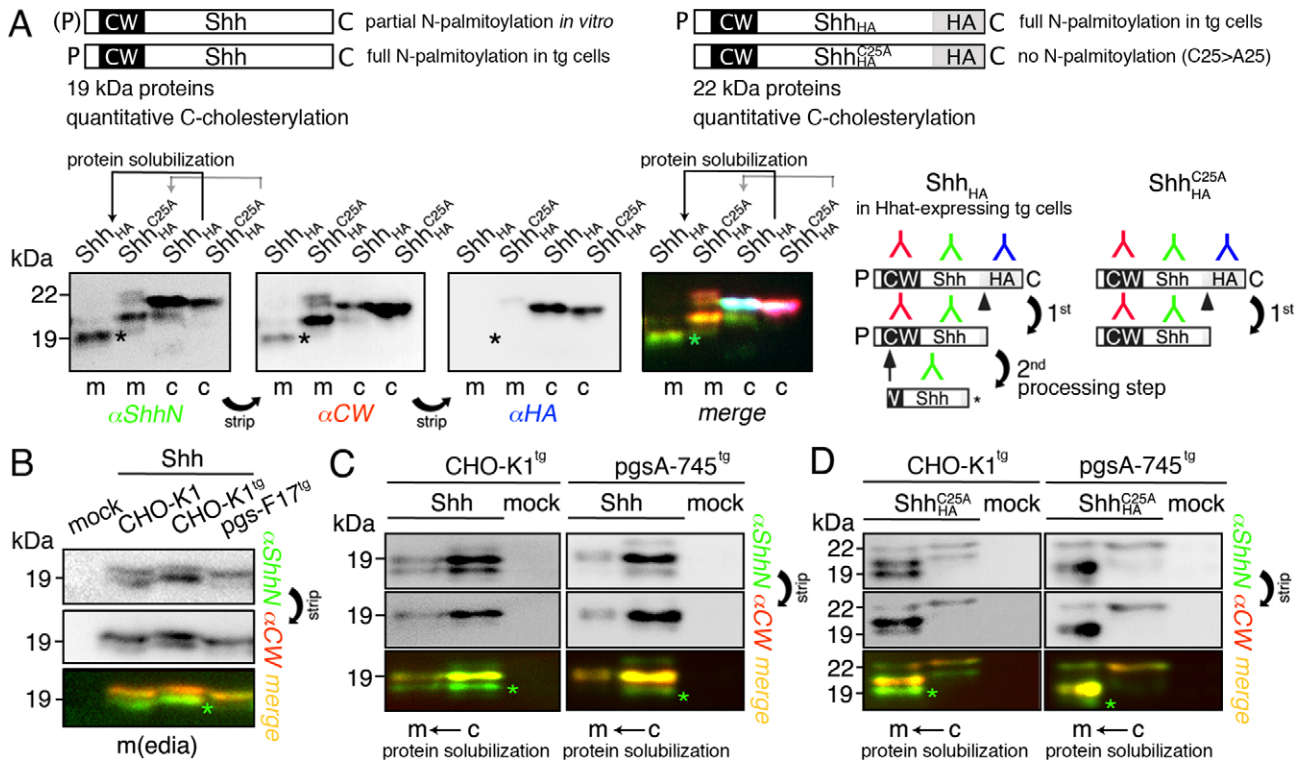

Fig. 2. Shh solubilization and processing from different HSPG-deficient CHO cell lines. (A) Top, Shh constructs used in this study. 'tg' cells co-express Hh acyltransferase (Hhat) to increase Shh N-palmitoylation [denoted by (P) or P]. C, cholesterol; CW, Cardin-Weintraub motif; HA, hemagglutinin tag. Lower left, processing of lipidated terminal Shh peptides during release. Palmitoylated Shh–HA due to Hhat coexpression, and non-palmitoylated (C25A) proteins were expressed in Bosc23 cells and the cellular (c) and corresponding soluble fractions (m) were analyzed by immunoblotting. To better demonstrate Shh processing during release, gray scale blots were inverted and colored [green, anti-Shh signal (αShhN); red, anti-Cardin–Weintraub signal (αCW); blue, anti-HA signal (αHA)]. Bright cellular signals in merged blots denote unprocessed proteins, yellow signals denote C-processed/N-unprocessed soluble proteins, and green signals confirm the removal of N- and C-terminal peptides. Solubilized Shh–HA was bound by polyclonal anti-ShhN antibodies but not by anti-Cardin–Weintraub and anti-HA antibodies. N-terminal processing of HA-tagged Shh^{C25A} was strongly impaired, as indicated by the predominance of C-terminally processed proteins (yellow band) (Jakobs et al., 2014). Lower right, models of C- and N-terminal Shh processing. Antibody-binding sites, N-palmitate (P), C-cholesterol (C), and cleavage sites (arrow, arrowhead) are indicated. (B) 19-kDa lipidated Shh was expressed in CHO-K1 cells and in Hhat-transfected CHO-$K1^{tg}$ and pgsF-17^{tg} cells, and protein shedding into the media was enhanced by 600 µg/ml MβCD. Hhat co-expression increased N-terminal Shh processing into a soluble protein of slightly reduced size in CHO-$K1^{tg}$ cells (asterisk), but not in pgsF-17^{tg} cells. (C) Shh solubilization from CHO-$K1^{tg}$ and pgsA-745^{tg} cells. Shh was not efficiently released from either cell line if compared to protein amounts in the cellular material, and N-terminal Shh processing in pgsA-745^{tg} cells was further reduced (asterisk). Compare soluble material in medium (m) with the corresponding cell-surface-associated material (c). (D) Increased relative amounts of unpalmitoylated HA-tagged Shh^{C25A} processing products, if compared to Shh in C, were released into the medium. Furthermore, N-terminal processing (asterisk), but not C-terminal processing, was strongly impaired in pgsA-745^{tg} cells. Scube2-conditioned medium was employed in all experiments; one representative result of three independent experiments is shown.

non-palmitoylated Shh^{C25A} expressed in Bosc23 cells (Fig. 2A), a HEK293-derived cell line commonly used to analyze Shh production and release. To monitor C-terminal Shh processing, we tagged both proteins with hemagglutinin (HA), resulting in the extended C-terminal membrane anchor N^{190}SVAAKSG-*YPYDVPDYA*-G^{198} (G198 represents the cholesterol-modified glycine; underlined italicized letters represent the tag) (Jakobs et al., 2014). To confirm N-terminal processing during release, we used anti-Cardin–Weintraub antibodies raised against the Cardin–Weintraub peptide K^{33}RRHPKK^{39} located adjacent to the palmitoylated cysteine residue (Ohlig et al., 2012). Polyclonal anti-ShhN antibodies were used to detect both full-length and truncated proteins on the same (stripped) blot (schematic in Fig. 2A). As expected, cellular Shh–HA was converted into soluble morphogens lacking most anti-Cardin–Weintraub and all anti-HA antibody binding (Fig. 2A, asterisk). Cell-surface-associated HA-tagged Shh^{C25A} was converted into a C-terminally processed, but N-terminally unprocessed soluble form (yellow band), showing that the N-terminal processing of unpalmitoylated morphogens was impaired (Ohlig et al., 2012). Consistent with our previous observation that Shh palmitoylation *in vitro* is incomplete (Jakobs et al., 2014), Shh processing in CHO-K1 cells was strongly enhanced after stable hhat transfection (CHO-$K1^{tg}$ cells, Fig. 2B, asterisk). These results demonstrate that both Hh lipidations contribute to Hh association with the cell membrane (Chamoun et al., 2001; Konitsiotis et al., 2014; Ohlig et al., 2011) to ensure that only fully processed Hh is released (Ohlig et al., 2012). This raises the question of how Hh shedding is controlled.

On the basis of previously described Hh colocalization with cell-surface glypicans prior to their release (Ayers et al., 2010; Vyas et al., 2008), we hypothesized that HSPGs might play this role. Consistent with this hypothesis, we observed that heparan sulfate expressed on the surface of 2-O sulfotransferase-deficient CHO-pgsF-17^{tg} cells (Xu and Esko, 2014) interfered with N-terminal Shh processing in the presence of 600 µg/ml methyl-β-cyclodextrin (MβCD), a cyclic oligosaccharide that activates sheddases and thus forces proteolytic processing of membrane-associated proteins (Fig. 2B) (Murai et al., 2011). The assembly of heparan sulfate in

Journal of Cell Science (2015) 128, 2374-2385 doi:10.1242/jcs.170670

these and other cells is not template driven; rather, it is thought to depend on the organization and specificity of biosynthetic enzymes and the availability of precursors. Thus, 2-O sulfotransferase deficiency not only reduces heparan sulfate 2-O-sulfation, but also strongly enhances N-sulfation and moderately elevates 6-O-sulfation by an unknown compensatory mechanism (Axelsson et al., 2012). These secondary biosynthetic effects lead to complex changes in the heparan sulfate domain structure and overall heparan sulfate sulfation in these cells. N-terminal Shh processing was also impaired in pgsA-745^{tg} cells, a mutant CHO cell line defective in heparan sulfate and chondroitin sulfate biosynthesis (Fig. 2C). In contrast, comparable Shh^{C25A} processing from CHO-K1^{tg} wild-type cells and pgsA-745^{tg} cells revealed that C-terminal proteolysis was largely heparan sulfate independent, at least in the presence of the tag (Fig. 2D). From this observation, we draw two major conclusions. First, that glycosaminoglycans, probably of the heparan sulfate kind, regulate Shh processing. Second, N-terminal processing is rate limiting in Shh release. The latter conclusion is supported by the detection of increased soluble product amounts from non-palmitoylated Shh^{C25A} in comparison to palmitoylated protein products (compare relative amounts of soluble and cellular material produced in CHO-K1^{tg} cells; Fig. 2C,D, left lanes) and the findings of others (Chamoun et al., 2001; Konitsiotis et al., 2014). Finally, we confirmed that Hh palmitoylation is not a strict prerequisite for N-terminal processing, because N-truncated Shh^{C25A} was detected in CHO-K1^{tg} but not in heparan sulfate-deficient cells (Fig. 2D, left, asterisk). The possibility that pgsA-745^{tg} cells lack sheddase expression was ruled out by reverse transcription PCR (RT-PCR), which revealed robust ADAM10 and ADAM12 expression in all cell lines (data not shown). C-terminal Shh processing in these cells also confirmed sheddase expression (Fig. 2D).

HSPG core proteins play only minor roles in Shh processing and release

Vertebrates express six Gpc family members (Gpc1–Gpc6) that stimulate or suppress Hh function in receiving cells, depending on the Gpc isoform (Capurro et al., 2008; Li et al., 2011). We therefore tested whether Gpc proteins in producing cells can also regulate Shh shedding in an isotype-specific manner. First, we expressed Shh alone in CHO-K1 cells or CHO-K1^{tg} cells as a control and quantified relative Shh amounts in media. As shown in Fig. 3A (Step 1), most Shh released from Hhat-transfected CHO-K1^{tg} cells was N-terminally processed, as demonstrated by a size shift and strongly impaired anti-Cardin–Weintraub antibody binding (center column, center row, right lane). In contrast, most solubilized

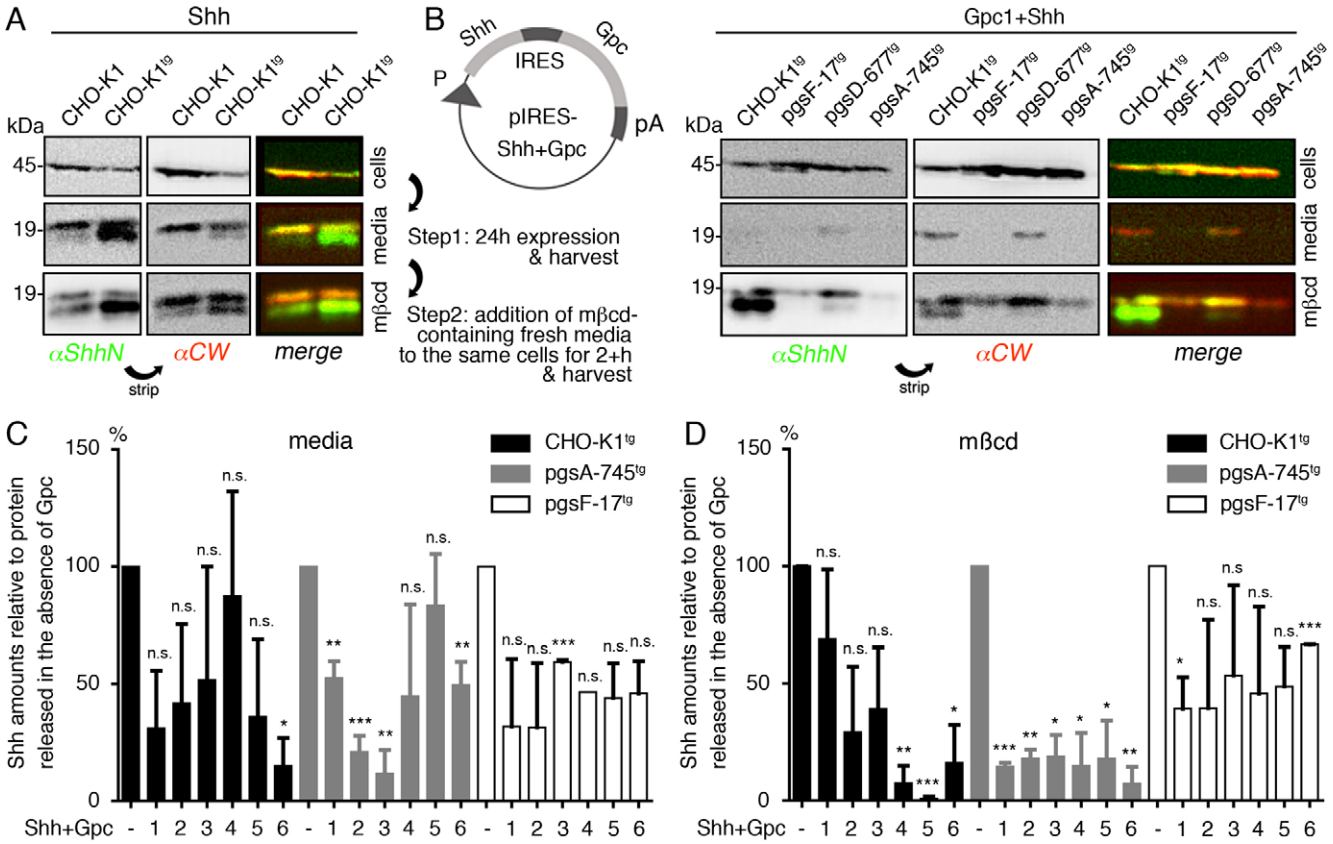

Fig. 3. HSPG-controlled variation in Shh expression and release. (A) Shh expression and release from CHO-K1 cells compared with that from stably Hhat-transfected CHO-K1^{tg} cells. CHO-K1^{tg} cells released most Shh in the N-terminally processed form, whereas most Shh from CHO-K1 cells was N-terminally intact (center row). MβCD-induced forced shedding was used to quantify the previously unreleased material (bottom). (B) pIRES-coupled Shh and Gpc expression. Shh translation from bicistronic mRNA was CAP dependent, whereas Gpc translation was CAP independent. P, promotor; IRES, internal ribosomal entry site. Gpc proteins suppressed Shh release in all CHO^{tg} cell lines (center row), but not its secretion to the cell surface, because morphogens were released by MβCD (bottom row). MβCD released only small amounts of N-terminally processed Shh from pgsF-17^{tg} and pgsA-745^{tg} cells. (C,D) Gpc1–Gpc6 and Shh were co-expressed in CHO-K1^{tg}, pgsA-745^{tg} and pgsF-17^{tg} cells and the soluble Shh obtained in the absence (C) or presence (D) of 600 µg/ml MβCD was quantified. In all three cell lines, Gpcs decreased Shh expression into serum-free medium to variable degrees. Proteins released in the absence of the Gpc were set to 100%. n=2 for CHO-K1^{tg} and pgsF-17^{tg} cells, n=3 for pgsA-745^{tg} cells. *P<0.05; **P<0.01; ***P<0.0001; n.s., not significant (P>0.05).

Journal of Cell Science (2015) 128, 2374-2385 doi:10.1242/jcs.170670

proteins produced in Hhat-untransfected cells remained N-terminally unprocessed (left lanes). Again, both observations confirm that palmitate tethers Hh to the cell membrane and thereby prevents the release of N-terminally unprocessed lipidated protein termini. To quantify the amounts of unreleased surface-associated Shh, we added fresh media containing 600 µg/ml MβCD to the same cells (Fig. 3A, Step 2). MβCD solubilized substantial amounts of previously unreleased protein from the surface of CHO-K1^{tg} cells in the same (N-truncated) form, whereas only small amounts of remaining unpalmitoylated Shh were released from Hhat-untransfected CHO-K1 cells (bottom). These findings show that Shh shedding at the cell surface is strictly controlled and that this control involves the lipidated N-terminal Shh peptide.

To analyze Gpc functions in this controlled process in detail, we next expressed Shh and Gpc1 from a bicistronic mRNA in CHO-K1^{tg} cells (Fig. 3B). Under serum-free conditions, we found that Gpc1 strongly impaired Shh release in comparison to the control Shh expressed in its absence (compare Fig. 3A,B, center rows), despite comparable Shh production (Fig. 3A,B, top rows). The addition of MβCD revealed that the unreleased material resided on the cell surface (Fig. 3B, bottom row). Shh release was also strongly impaired in Gpc1 and Shh co-transfected pgsF-17^{tg} cells, pgsA-745^{tg} cells, and a CHO cell line deficient in heparan sulfate but not chondroitin sulfate biosynthesis (pgsD-677^{tg} cells). The observation that not even MβCD released N-terminally processed proteins from these mutant cells supported the hypothesis that the presence of properly modified heparan sulfate is required for Shh solubilization from the cell surface. Fig. 3C extends these findings, showing quantified soluble Shh co-expressed with Gpc1–Gpc6 from CHO-K1^{tg}, pgsF-17^{tg} cells and pgsA-745^{tg} cells relative to the material expressed in the absence of exogenous Gpcs. We observed that Shh solubilization as a consequence of Gpc1–Gpc6 co-expression was variably reduced in all cell lines (Fig. 3C). This finding indicates that most Gpcs suppress Shh shedding under serum-free conditions (Fig. 3C) as well as in the presence of MβCD (Fig. 3D). Finally, we determined that the solubilized morphogens showed similar activities in the Shh-responsive cell line C3H10T1/2 (Nakamura et al., 1997), indicating that Gpc isoforms do not impact upon Shh biofunction in receiving cells (supplementary material Fig. S1).

Shh and Gpc coexpression was also analyzed in Bosc23 cells. We first determined that Gpc2 and Shh, and Gpc6 and Shh expression levels and protein colocalization on the cell surface were comparable (Fig. 4, see yellow punctate staining in D and H) (Vyas et al., 2008). Next, we isolated cell lysates and supernatants from pIRES-Shh-Gpc-transfected Bosc23 cells and analyzed cellular and solubilized Shh by SDS-PAGE and immunoblotting as described above. Fig. 5 shows that the Shh solubilization was mostly unchanged after normalization of protein production rates to the Shh control level. With the exception of Gpc2, our findings confirm that the Gpc core proteins play only minor roles in the regulation of Shh release from Bosc23 cells. Both findings suggest that direct Shh–heparan-sulfate interactions represent the main determinant for Shh release. Alternatively, Gpc knockdown or overexpression might affect Shh release by modulating indirect changes in sheddase expression (Purushothaman et al., 2008).

Proteolytic processing does not depend on terminal Shh lipids

To distinguish between these two possibilities, we analyzed heparan-sulfate-regulated Shh processing under cell-free conditions. Preliminary results revealed that non-lipidated ShhN^{C25S} was processed in CHO-K1^{tg} cells but not in pgsA-745^{tg} cells (supplementary material Fig. S2), suggesting that heparan-sulfate-regulated Shh processing can also occur independently of Hh membrane association. We confirmed lipid-independent protein processing in detail by comparing cellular and solubilized forms of Shh and C-terminally hexahistidine-tagged ShhN (ShhN–His$_6$) (Fig. 6A). Shh and ShhN–His$_6$ were transfected into Bosc23 cells, expressed in [9,10(n)-^{3}H] palmitic acid containing serum-free medium, concentrated by heparin-sepharose pulldown, and blotted onto polyvinylidene difluoride (PVDF) membranes for SDS-PAGE, immunoblotting, and autoradiography analysis of the same blot. As expected, a fraction of soluble 19-kDa Shh generated from the cell-

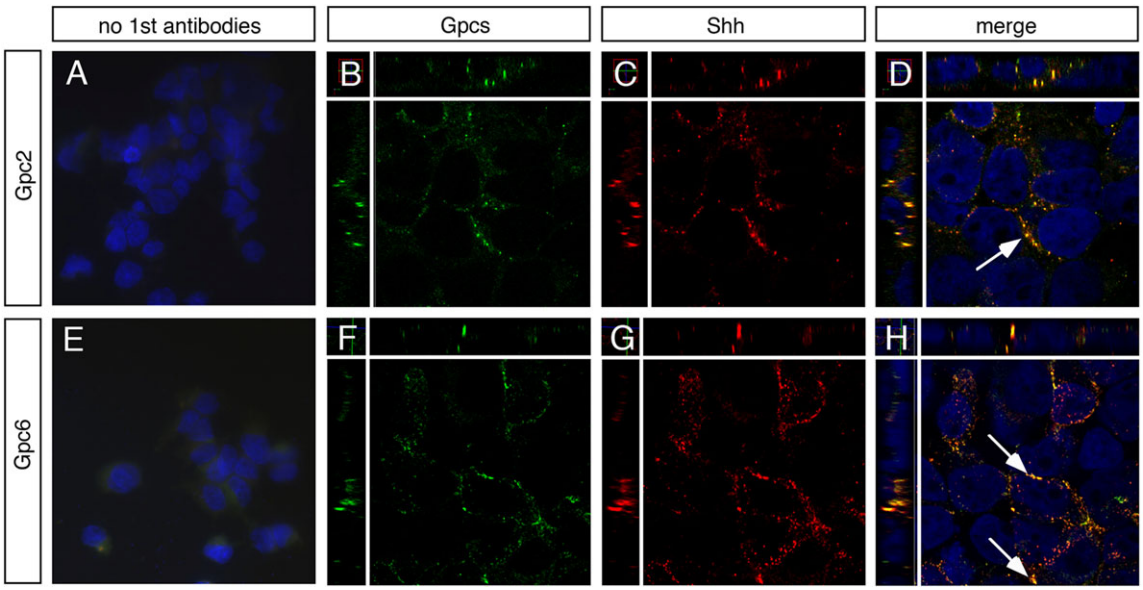

Fig. 4. Gpcs associate with Shh at the cell surface. Gpc2 (B) and Gpc6 (F) were co-expressed with Shh (C,G) in Bosc23 cells. Cells were antibody-stained under non-permeabilizing conditions. Pearson's threshold correlation coefficients for Shh and Gpc2, and Shh and Gpc6 of 0.65 and 0.74 indicate significant colocalization, as visualized in the merged figures (D,H, yellow staining, arrows). Blue: nuclei (A,E).

Journal of Cell Science (2015) 128, 2374-2385 doi:10.1242/jcs.170670

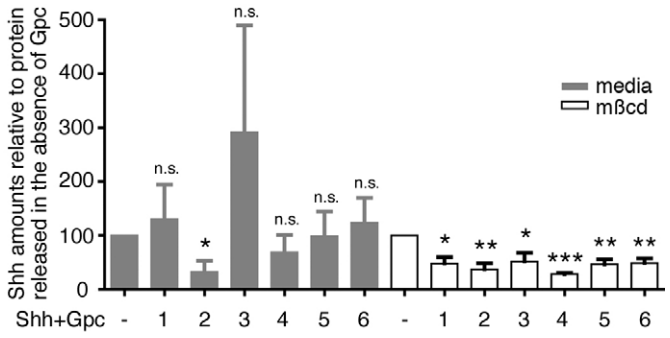

Fig. 5. Shh release and biofunction is regulated by Gpcs. Gpc1–Gpc6 and Shh were co-expressed in Bosc23 cells from bicistronic mRNA, and the cellular material and soluble proteins obtained in the presence or absence of 600 µg/ml MβCD were quantified. Normalization of soluble Shh to cellular expression levels shows that Gpc1–Gpc6 do not significantly differ in their ability to solubilize Shh in the absence of MβCD (with the exception of Gpc2, 33%±21 of Shh expression in the absence of exogenous Gpc, P=0.033, n=3), and significantly reduce Shh solubilization in the presence of MβCD (Gpc1 50%±11, P=0.01; Gpc2 37%±11, P=0.005; Gpc3 52%±15, P=0.036; Gpc4 28%±2, P=0.0001; Gpc5 46%±9, P=0.004 and Gpc6 49%±9, P=0.046, respectively, n=3). *P<0.05, **P<0.01, ***P<0.0001. Values are mean±s.d. percentages relative to the Gpc-untransfected control (–), which was set at 100%.

tethered precursor was processed, as indicated by a molecular mass shift and associated loss of the radiolabel (Fig. 6A, left, asterisk). Another soluble protein fraction represented by an upper medium band also lacked the radiolabel, demonstrating that this fraction does not simply represent cellular (lipidated) material that was leaked into the medium or released by some other means (Creanga et al., 2012; Palm et al., 2013). Instead, most of these proteins represent Shh that escaped N-palmitoylation during biosynthesis and were therefore released in an N-terminally unprocessed (but C-terminally processed) form. This result is supported by the observation of processing products obtained from 28-kDa ShhN–His_6. A fraction of this protein was N-terminally processed, as indicated by a small size shift and the absence of the radiolabel (Fig. 6A, right, arrow). Alternatively, ShhN–His_6 was C-terminally processed into 19-kDa ShhN, as indicated by the substantial size shift and the presence of the radiolabel (Fig. 6A, right, arrowhead). Combined N- and C-terminal processing removed both peptides and produced a protein that was indistinguishable from fully processed Shh (asterisks). This finding confirms that neither N-terminal Shh palmitoylation nor C-terminal cholesterylation are essential prerequisites for proteolytic Shh maturation under the conditions used in this assay, allowing us to expand our analysis of ShhN–His_6 processing *in vitro*.

Heparan sulfate potentiates Shh processing

As stated earlier, we hypothesized that Gpc heparan sulfate chains act as assembly sites for proteases and their substrates, in turn bringing them into close proximity to facilitate substrate turnover. To test this idea, we harvested and centrifuged 19-kDa Shh and 28-kDa ShhN–His_6 expressed into serum-free Dulbecco's modified

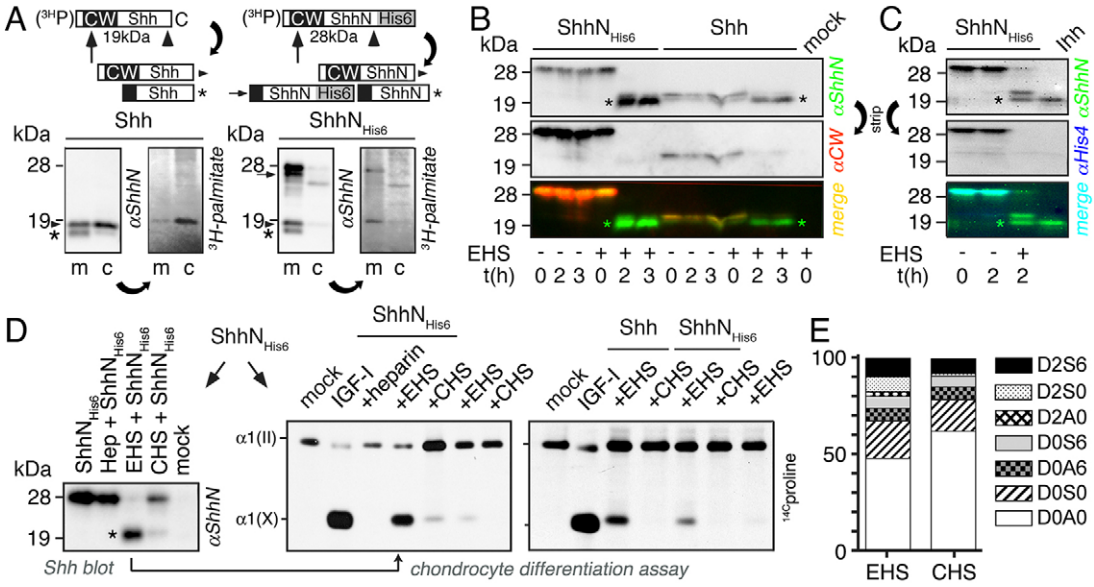

Fig. 6. Heparan sulfate regulates the processing of lipidated and unlipidated Shh. (A) Top, schematic of processed and unprocessed hexahistidine-tagged, non-cholesterylated ShhN–His_6 and dual-lipidated Shh. N-terminal (arrow) and C-terminal (arrowhead) processing sites are indicated. Expected products of single or combined (*) cleavage are also shown. Bottom, immunoblot (left) and autoradiograph (right) of [9,10(n)-^{3}H] palmitic-acid-labeled, full-length Shh and ShhN–His_6 in cell lysates (c) and media (m). Fully processed 19-kDa Shh (bottom band) was detected in media. In contrast, the cellular material was not processed, as indicated by ^{3}H-autoradiography. Unprocessed, N-terminally processed (arrow), C-terminally processed (arrowhead), and dually processed (*) ShhN–His_6 were also detected. (B) EHS potentiated specific conversion of Shh and 28-kDa ShhN–His_6 into the same dual-processed 19-kDa products (*). In the absence of EHS, proteins remained unprocessed, whereas co-incubation with 20 µg/ml EHS induced complete N- and C-terminal processing, as indicated by a size shift and abolished anti-Cardin–Weintraub (αCW) antibody binding. (C) Processed 19-kDa proteins derived from 28-kDa ShhN–His_6 lack hexahistidines and correspond in size to endogenous Ihh secreted from cultured chick chondrocytes. (D) Truncated Shh is bioactive. Left, ShhN–His_6 was incubated with 20 µg/ml EHS, cancer-cell heparan sulfate (CHS) or heparin. After 2 h, proteins detected in the absence of exogenous heparan sulfate or in the presence of heparin (Hep+$ShhN_{His6}$) remained unprocessed. In contrast, EHS co-incubation resulted in specific ShhN–His_6 processing. Processed proteins induced chondrocyte differentiation, as indicated by a switch from collagen II to collagen X [α1(X)] production (right). Heparin- and CHS-incubated proteins were inactive, and EHS and CHS alone were also inactive (two right lanes). IGF-I-stimulated chondrocyte hypertrophy served as a positive control. (E) Heparan sulfate was isolated and samples digested with heparin lyases. The resulting disaccharides were analyzed by quantitative LC-MS. Values denote the mean percentage of total disaccharide. The abbreviations used denote the following disaccharides: D0A0 (ΔUA1,4GlcNAc), D0S0 (ΔUA1,4GlcNS), D0A6 (ΔUA1,4GlcNAc-6S), D0S6 (ΔUA1,4GlcNS-6S), D2A0 (ΔUA2S1,4GlcNAc), D2S0 (ΔUA2S1,4GlcNS) and D2S6 (ΔUA2S1,4GlcNS-6S).

Journal of Cell Science (2015) 128, 2374-2385 doi:10.1242/jcs.170670

Eagle's medium (DMEM), and we incubated the soluble proteins with pooled glycosaminoglycans isolated from E12.5–E18 mouse embryos (EHS). EHS was used because of its essential role in Hh signaling *in vivo* (Grobe et al., 2005; Pallerla et al., 2007; Yasuda et al., 2010). After EHS-conditioned media were incubated for 0–3 h at 37°C to allow for protease–substrate assembly and Shh processing, samples were precipitated with trichloroacetic acid (TCA) and analyzed by SDS-PAGE and immunoblotting as described above. Consistent with our expectations, both proteins were not processed in the absence of exogenous EHS (Fig. 6B, 0 to 3 h), but EHS potentiated Shh and ShhN–His_6 processing by an unidentified Bosc23 protease. The 28-kDa ShhN–His_6 form was converted into 19-kDa proteins lacking C-terminal hexahistidines and the N-terminal Cardin–Weintraub peptides (asterisks). These proteins were comparable in size to processed Shh and bioactive Ihh endogenously secreted from cultured chick chondrocytes (Fig. 6C) (Dierker et al., 2009). This result demonstrates that lipidated and non-lipidated Shh was processed by similar, or the same, proteolytic enzyme(s) (Fig. 6C, asterisk) and that heparan sulfate potentiates processing of both proteins in a direct way.

The heparan sulfate source determines Shh processing

We next compared biological activities of truncated and unprocessed soluble proteins. Supernatants of ShhN–His_6-expressing Bosc23 cells were incubated with 20 µg/ml heparin, EHS, or mixed heparan sulfate derived from B16-F1 and PC-3 cancer cell lines (CHS) as an approximation of Shh-sensitive pancreatic and skin cancers. We observed that heparin was inactive and that CHS aided the conversion of ShhN–His_6 into an unstable product (Fig. 6D, blot). As shown earlier, EHS enhanced the conversion of 28 kDa ShhN–His_6 into bioactive 19 kDa proteins (Fig. 6D, chondrocyte assay) (Dreier et al., 2008). In this bioassay, supernatants from mock-transfected Bosc23 cells were inactive, as were heparin- and CHS-treated samples. Insulin-like growth factor I (IGF-I) served as a positive control, and EHS alone was inactive. The same was observed for Shh (Fig. 6B,D). We draw two conclusions from these findings. First, that ShhN–His_6 processing increases Shh biofunction (Ohlig et al., 2011), and, second, that ShhN–His_6 processing depends on the source of heparan sulfate (as supported by results shown in supplementary material Fig. S2B). Quantitative disaccharide analysis of heparin-lyase-digested heparan sulfate by liquid chromatography electrospray ionization tandem mass spectrometry (LC-Esi-MS/MS) (Lawrence et al., 2008) revealed that overall EHS sulfation (0.86 sulfates per disaccharide) was increased over that of CHS (0.6 sulfates per disaccharide) (Fig. 6E). Variances in overall charge and disaccharide composition of EHS and CHS are consistent with, and likely the cause of, the observed differences in Shh processing.

Heparan sulfate regulates Shh release from pancreatic cancer cells

Ligand-dependent activation of Hh signaling is associated with tumorigenesis in a subset of epithelial cancers, including colon, pancreatic and ovarian cancer (Theunissen and de Sauvage, 2009), and HSPGs regulate Shh activity and Shh-dependent cancer cell proliferation (Chan et al., 2009). Importantly, Hh does not activate autocrine cancer cell signaling, but instead signals to the stromal compartment (Tian et al., 2009; Yauch et al., 2008), which in turn provides a more favorable environment for tumor growth. RT-PCR analysis of the pancreatic tumor cell line PANC1 confirmed the expression of components required for Shh production and release, but not for Hh reception (supplementary material Fig. S3). This observation is in line with the described shedding of endogenous Shh from the PANC1 cell surface (Damhofer et al., 2015). We confirmed Shh–HA shedding from PANC1 cells by the nonphysiological and physiological release factors MβCD and Scube2, as indicated by enhanced electrophoretic product mobility in comparison to the cell-bound protein precursor (Fig. 7A). Importantly, adding 'processing-active' heparan sulfate isolated from CHO-K1 cells and E12.5 mouse embryos to Shh-expressing PANC1 cells also increased Shh–HA processing and solubilization (Fig. 7A). We further observed that 14 µg/ml heparan sulfate isolated from tumor cell lines B16 Bl6, B16 F1, PC3 and HeLa, or heparan sulfate from different mouse embryos, stimulated Shh processing to different extents (Fig. 7B). Heparan sulfate isolated from PC3 and B16 cells, as well as from E12.5 and E14.5 mouse embryos, potentiated Shh shedding from PANC1 cells, whereas HeLa-derived heparan sulfate and heparan sulfate isolated from E14.5 and Sulf-deficient mouse embryos was inactive. Notably, 6-O

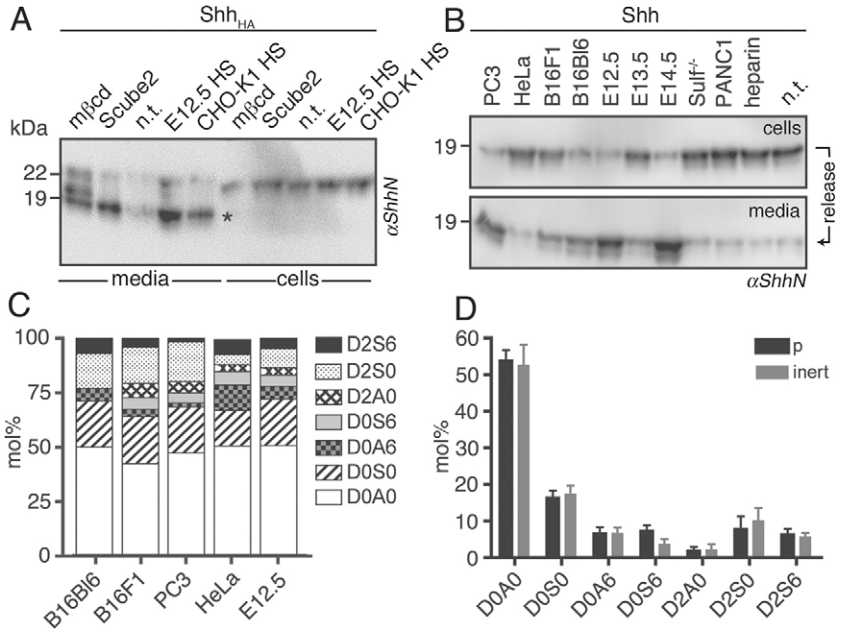

Fig. 7. Heparan sulfate regulates Shh release from PANC1 pancreatic cancer cells. (A) MβCD, Scube2 and heparan sulfate facilitate the specific conversion of cellular 22-kDa Shh–HA into soluble 19-kDa products (asterisk). (B) Heparan-sulfate-regulated Shh release depends on the source of heparan sulfate. Heparan sulfate isolates from various tumor cell lines and from mouse embryos stimulated Shh–HA processing and release to different extents. Sluf$^{-/-}$, Sulf1 and Sulf2 double-null; n.t., not treated. (C) Heparan sulfate was isolated from cancer cell lines and E12.5 mouse embryos and samples were digested with heparin lyases. The resulting disaccharides were analyzed by quantitative LC-MS; values denote the mean percentage of total disaccharide (abbreviations are as in Fig. 6E). (D) Pooled relative disaccharide amounts in processing-active heparan sulfate (p, such as PC3 heparan sulfate) or inactive heparan sulfate (inert, such as HeLa heparan sulfate) do not reveal any specific 'disaccharide signature'.

Journal of Cell Science (2015) 128, 2374-2385 doi:10.1242/jcs.170670

oversulfated heparan sulfate isolated from Sulf1 and Sulf2 double mutant mouse embryonic feeder cells was also inactive. Heparin and PANC1 heparan sulfate served as negative controls. These findings reveal that heparan sulfate, depending on its source, acts as a new Shh release stimulator in cultured pancreatic cancer cells.

Lack of characterizing 'signature disaccharides' in active heparan sulfate

To determine whether specific heparan sulfate sulfations and Shh release are linked, we conducted disaccharide analysis of our heparan sulfate isolates (Fig. 7C,D). We found that overall heparan sulfate sulfation of 'processing (p)-active' heparan sulfate isolates varied considerably: 0.8 sulfates per disaccharide for PC3 heparan sulfate, 0.86 sulfates per disaccharide for B16 F1 heparan sulfate, and 0.82 sulfates per disaccharide for B16Bl6 heparan sulfate; 0.73 sulfates per disaccharide for E12.5 heparan sulfate and 0.73 sulfates per disaccharide for E14.5 heparan sulfate. 'Inert' HeLa heparan sulfate contained 0.73 sulfates per disaccharide, heparan sulfate from Sulf1- and Sulf2-null mouse embryonic feeder cells contained ~1 sulfate per disaccharide (Lamanna et al., 2006), and heparin contained ~2 sulfates per disaccharide. Thus, we found no correlation between overall heparan sulfate sulfation and its ability to stimulate Shh-processing from PANC1 cells. Quantitative disaccharide analysis also failed to reveal any specific 'signature' disaccharide in active versus inactive heparan sulfate (Fig. 7C,D).

DISCUSSION

Tissue patterning and growth in development is a dynamic process that depends on the tight control of spatiotemporal morphogen production, spread and reception. Our work emphasizes the key role of Gpcs in the regulation of Hh release from producing cells and tissues *in vitro* and *in vivo*. Gpcs are heparan-sulfate-modified proteins that are bound to the outer surface of the plasma membrane through their GPI anchors. This leads to their association with lipid rafts (Mayor and Riezman, 2004), specialized membrane microdomains that serve as organizing centers for the assembly and trafficking of multiple signaling molecules and their receptors. Notably, because of their N-terminal palmitoylation and C-cholesterylation, Hh proteins also cumulate in lipid rafts (Resh, 2006; Rietveld et al., 1999) and aggregate with Gpcs (Vyas et al., 2008). This suggests that GPI-linked HSPGs on the surface of producing cells act as storage sites for Hh morphogens. Subsequent Hh solubilization depends on the proteolytic processing of lipidated terminal peptides because the extraction of even a single cholesterol molecule from a lipid bilayer requires free energies ranging from 60–90 kJ/mol (Bennett et al., 2009), decisively preventing the discharge of lipidated Hh proteins. Alternative membrane-coupled Hh transport by transcytosis, cytonemes or exosomes is incompatible with the one-way route taken by authentic, dual-lipidated and multimeric Shh to the cell surface but not back into the cell (Gao and Hannoush, 2014).

How is Hh and HSPG assembly linked with subsequent proteolytic Hh release? One attractive idea is that not only do Gpcs serve as platforms for Hh assembly and storage, but they also associate with Hh release factors, such as Hh sheddases (Dierker et al., 2009) or the sheddase activator Scube2 (Jakobs et al., 2014) (Fig. 8). Indeed, we show that sheddase function and specificity can be achieved in two heparan-sulfate-regulated ways. First, extracellular heparan sulfate, depending on its site of production, might activate or attract sheddases to Shh morphogens already bound to these chains. This finding is supported by the observed absence of (N-terminal) Shh processing in heparan sulfate-deficient cells and the potentiation of Shh processing by exogenous heparan sulfate *in vitro*. Hh sheddase activation by heparan sulfate is further consistent with the known increase of Hh solubilization by Suramine, a polysulfated compound (Etheridge et al., 2010) and with Syndecan 2 (another cell surface HSPG) acting as a docking receptor and activator for MMP7 (Ryu et al., 2009). Moreover, ADAM12 associates with HSPGs through its cysteine-rich domain (Iba et al., 2000), and heparan sulfate binding to ADAM12 transiently activates the enzyme (Sorensen et al., 2008). Finally, heparin activates MMP2 and MMP9 through MT-1 (Butler et al., 1998) and heparan sulfate also activates MMP2 (Koo et al., 2010). Notably, we observed pro-MMP9 (but not pro-MMP2) activation by the same heparan sulfate found to be active in Shh release (U.P., unpublished observations). The soluble protease(s) involved in Shh processing in our assays, however, remain to be identified.

Binding of heparan sulfate chains to the Cardin–Weintraub cleavage site might constitute a second level of processing control (Fig. 8). Consistent with this possibility, heparan sulfate strongly interacts with Shh (Carrasco et al., 2005; Farshi et al., 2011; Zhang et al., 2007) and did not potentiate its processing, and heparin dose-dependently blocked Shh processing and release (supplementary material Fig. S4). Examples for other highly charged, inactive glycosaminoglycans are pgsF-17 heparan sulfate and heparan sulfate isolated from Sulf1- and Sulf2-null mouse embryonic feeder cells, which both show significantly increased heparan sulfate 6-O sulfation (Bai and Esko, 1996; Lamanna et al., 2006). *In vivo* and *in vitro*, heparan sulfate 6-O sulfate at the cell surface is removed by the activity of soluble 6-O sulfatases (Sulfs): lack of Sulf activity therefore leads to heparan sulfate oversulfation (enhancing the Cardin–Weintraub interactions with heparan sulfate), whereas Sulf gain-of-function reduces heparan sulfate 6-O sulfation and charge (loosening Hh interactions). Notably, removal of Sulf1 in the posterior Hh-producing *Drosophila* wing compartment significantly impaired Hh signaling (Zhang et al., 2007), and concomitant Sulf1 overexpression extended the Hh gradient (Wojcinski et al., 2011). In the vertebrate neural tube, Shh-producing cells must also upregulate Sulf1 to reach

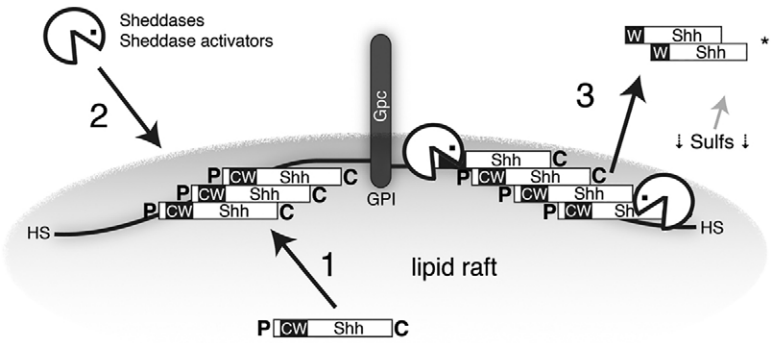

Fig. 8. Schematic of two-way Shh release by glypican HSPGs. Initially, Hh proteins tethered to the cell surface assemble into Gpc-associated heteroprotein hubs (1; Vyas et al., 2008). We suggest that, through their heparan sulfate chains, Shh and Gpc hubs subsequently attract or activate proteins required for Hh release (2), such as sheddases and sheddase activators. The decision to release Shh then depends on the degree of heparan sulfate sulfation of the functional release complex – Shh cleavage occurs under the condition that heparan sulfate does not block access to the Cardin–Weintraub sheddase target site (3), but cleavage might be impaired by increased electrostatic Shh–heparan-sulfate interactions, for example, as a consequence of Sulf inactivity. In the latter case, the unprocessed morphogen clusters remain 'trapped' at the cell surface. P, palmitate; C, cholesterol.

Journal of Cell Science (2015) 128, 2374-2385 doi:10.1242/jcs.170670

their full inductive potential, confirming that Sulf1 stimulates Shh activation by decreasing heparan sulfate 6-O sulfation at the ligand source (Oustah et al., 2014). We support these observations and suggest that they can be explained by Sulf-regulated competitive heparan sulfate binding to the Cardin–Weintraub sheddase target site, which in turn impairs Hh processing and release.

Overall, our work, by characterizing Shh solubilization in response to HSPG expression and heparan sulfate modifications, reveals major Gpc functions in the switch between morphogen precursor accumulation at the cell surface and its release in processed form. To a large extent, this direct regulation depends on the charge of heparan sulfate and its domain structure controlling substrate accessibility. This raises the very important, yet poorly investigated question of how cells regulate heparan sulfate charge and structure because, unlike in the case of DNA, RNA and protein biosynthesis, the assembly of heparan sulfate is not template driven. Rather, heparan sulfate assembly seems to rely on 'ad hoc' integration of environmental clues to increase or decrease the frequency of binding sites, for example, through the expression of Sulf proteins. This raises the exciting possibility that the inherent, template-independent plasticity of heparan sulfate might also regulate sheddase activities and their substrate specificities in other developmental settings and in pathological conditions such as inflammation, cancer, rheumatoid arthritis and Alzheimer disease.

MATERIALS AND METHODS

Drosophila strains

Fly RNAi strains UAS-sfl-RNAi, UAS-dally-RNAi, UAS-dlp-RNAi, and UAS-ttv-RNAi were obtained from the Bloomington Drosophila Stock Center or from the Vienna Drosophila RNAi Center (Vienna Stock Center: dally3 #v14136, dlp2 #v100268; Bloomington Stock Center: dally1 #33952, dally2 #28747, dlp1 #34091). UAS-GFP-RNAi flies and en-GAL4 flies were kindly provided by Christian Klämbt, University of Münster, Germany. UAS-RNAi fly lines were crossed with en-Gal4 to suppress target gene expression under engrailed control in the Hh-expressing posterior compartment. Flies were maintained at 25°C, and RNAi expression experiments were conducted at 29°C. Right wings of adult F1 flies were mounted in Hoyers medium, photographed, and analyzed by MoticImage. Phenotypic changes in *Drosophila* wing patterning were quantified by dividing the L3–L4 intervein area by the L2–L3 intervein area (L3–L4/L2–L3).

Cloning and expression of recombinant Shh and glypicans

Shh constructs were generated from murine cDNA (NM 009170) by PCR using primers for the wild-type gene or primers carrying the desired point mutations and tag sequences. Secreted lipidated Shh (nucleotides 1–1314, corresponding to amino acids 1–438) was generated in Bosc23 cells [a human 293 T derivative, an embryonic kidney cell line (Zeng et al., 2001)], PANC1 cells (Damhofer et al., 2015) and CHO cells affected in their ability to synthesize heparan sulfate. Secreted unlipidated ShhN (nucleotides 1–594, corresponding to amino acid 1–198 of murine Shh) was also produced. PCR products were ligated into pGEM (Promega), sequenced and subsequently released and religated into pcDNA3.1 (Invitrogen) for the expression of lipidated 19-kDa Shh, or into pcDNA3.1/myc-HisC (Invitrogen) for the expression of soluble, C-terminally hexahistidine-tagged 28-kDa ShhN–His_6 (the large size is due to the presence of a c-Myc and intervening cloning sequence). Gpcs and Shh were cloned into pIRES for bicistronic expression of Shh (CAP dependent) and Gpc (CAP independent) in the same cells.

Cell culture

Bosc23 cells and PANC1 cells were cultured in DMEM (Gibco BRL) supplemented with 10% fetal calf serum (FCS) and 100 µg/ml penicillin-streptomycin. Cells were transfected by using PolyFect (Qiagen). Cells were grown for 36 h, washed with phosphate-buffered saline (PBS), and incubated in serum-free DMEM for various times in the presence or absence of stimulators or inhibitors of shedding, followed by ultracentrifugation at 210,000 ***g*** for 60 min to remove membrane-tethered Shh. Serum-free supernatants were TCA precipitated. Endogenously produced Ihh was isolated from chondrocytes derived from the cranial third of chick embryo sterna and cultured in agarose suspension cultures under serum-free conditions in the presence of 100 ng/ml insulin-like growth factor I (IGF-I) (Dreier et al., 2008). All procedures and protocols met the guidelines for animal care and experiments in accordance with national and European (86/609/EEC) legislation. Several CHO cells with defects in proteoglycan synthesis (pgs) were included in this study and compared with wild-type CHO K1 cells to analyze the effect of HSPGs on Shh. Lacking functional xylosyltransferase, the CHO cell line pgsA-745 is devoid of glycosaminoglycans (heparan sulfate and chondroitin sulfate). CHO pgsF-17 cells are defective in 2-O-sulfation of iduronic acid and GlcUA, which increases 6-O-sulfation (Bai and Esko, 1996). CHO pgsD-677 cells are defective in heparan sulfate, but not chondroitin sulfate biosynthesis (Lidholt et al., 1992), leading to increased compensatory chondroitin sulfate expression on the cell surface. Where indicated, CHO cell lines stably expressed Hhat to increase N-palmitoylation of recombinant Shh. Comparable Hhat expression was confirmed by RT-PCR. CHO cells were cultured in medium containing 50% DMEM and 50% DMEM/Hams F-12 (Lonza) in the presence of 10% FCS and 100 µg/ml penicillin-streptomycin. Where indicated, 600 µg/ml MβCD was added to serum-free medium. CHO cells were transfected by using PolyFect (Qiagen). At 24 h after transfection, cells were washed once with 1×PBS, and 1 ml of Scube2-conditioned serum-free medium was added to the cells. Media were harvested after another 24 h and processed. Based on the established role of Scube2 glycoproteins (signal sequence, cubulin domain, epidermal growth factor 2) in Hh release from 293 T cells (Tukachinsky et al., 2012), HEK293S cells (Creanga et al., 2012), and Bosc23 cells (Jakobs et al., 2014), Scube2-conditioned medium was used in all Shh release experiments.

Protein analysis

Proteins were resolved by 15% reducing SDS-PAGE and western blotted. Antibodies against ShhN (polyclonal goat IgG; R&D Systems), Cardin–Weintraub (R&D Systems), or HA were used for primary detection, and horseradish peroxidase (HRP)-conjugated donkey anti-goat IgG (detecting anti-ShhN), goat anti-rabbit IgG (detecting anti-Cardin–Weintraub), and goat anti-mouse IgG (detecting anti-HA) were used for secondary detection, followed by chemiluminescent analysis (Pierce) and signal quantification by ImageJ (http://rsb.info.nih.gov/ij/). In all Gpc coexpression analyses, data were plotted as released versus cell-bound Shh relative to the value obtained with the control, which was set to 100%. Radiolabeling was conducted as described previously (Ohlig et al., 2011). Briefly, 1 mCi [9,19(n)-^{3}H] palmitic acid was added to Shh-transfected Bosc23 cells in serum-free medium at 24 h after transfection, and cultured for an additional 40 h. [^{3}H] palmitic-acid-labeled cells were lysed, and cells and media were subjected to heparin–Sepharose pulldown to improve the signal-to-noise ratio. After SDS-PAGE and western blotting, PVDF-immobilized proteins were first immunodetected and membranes subsequently autoradiographed.

Confocal microscopy

Shh and HA-tagged Gpc-transfected cells were fixed and incubated at 4°C overnight with antibodies against Shh and the HA-tagged Gpc proteins. They were visualized by using a LSM 510 confocal microscope (Carl Zeiss, Jena, Germany). Thresholded Pearson's correlation coefficients were determined by Volocity.

Analysis of mRNA expression

For RT-PCR analysis in Bosc23 and PANC1 cells, RNA was isolated by using TriZol reagent (Invitrogen) and cDNA was generated with the First-Strand cDNA Synthesis Kit (Fermentas). Primer sequences used for PCR can be provided upon request.

Preparation and analysis of tissue heparan sulfate

Tissues or cells were digested overnight with 12 mg/ml pronase in 320 mM NaCl and 100 mM sodium acetate (pH 5.5) at 40°C, diluted 1:3 in water, and applied to 2 ml DEAE Sephacel columns. For disaccharide analysis, proteins attached to the glycosaminoglycans were β-eliminated overnight at 4°C (5 M

NaOH, 10 M $NaBH_4$), neutralized with acetic acid, and applied to a PD-10 (Sephadex G25) column (Pharmacia, Uppsala, Sweden). Columns were pre-equilibrated with 25 ml 10% ethanol and a 2.5 ml sample was loaded per column. Glycosaminoglycans were eluted with 10% ethanol, lyophilized, and resuspended in double-distilled water. For compositional disaccharide analysis, 10 µg glycosaminoglycan samples were first digested by using heparin lyases I, II and III (1.5 mU each in 100 µl reactions) (IBEX, Montreal, Canada) at 37°C for 1 h, and the resulting disaccharides were separated from undigested material by using a 3 kDa spin column (Centricon, Bedford, MA). Analysis was then carried out by liquid chromatography–mass spectrometry (LC-MS). Disaccharides were separated on a C18 reverse phase column (0.46×25 cm) (Vydac) with the ion-pairing reagent dibutylamine (Sigma), and eluted species were evaluated with a quantitative mass spectrometric method (Lawrence et al., 2008).

Shh-dependent differentiation of precursor cells

At 40 h post-transfection, supernatants from Shh and mock-transfected Bosc23 cells were harvested and added to C3H10T1/2 cells. Cyclopamine (2.5 µM), a specific inhibitor of Shh signaling, and the ShhN-neutralizing antibody 5E1 (Ericson et al., 1996) were added to confirm specificity of the assay. At 5–6 days after induction, cells were lysed (20 mM Hepes, 150 mM NaCl, 0.5% TritonX-100, pH 7.4) and Shh-induced alkaline phosphatase activity was measured after addition of 120 mM p-nitrophenolphosphate (Sigma) in 0.1 M glycine buffer (pH 10.4). Chondrocytes were isolated from the cranial third of 17-day-old chick embryo sterna and cultured for 14 days in agarose suspension culture under serum-free conditions in the presence (positive control) or absence of 100 ng/ml IGF-I. Shh-induced chondrocyte hypertrophy resulted in a switch from collagen II production to collagen X release.

Statistical analysis

All statistical analysis was performed in Prism by using a Student's *t*-test (two-tailed, unpaired, confidence interval 95%). All error estimates are s.d.

Acknowledgements

We thank Jeff Esko (UC San Diego, USA) for CHO cells; Dorothee Spillmann (Uppsala University, Sweden) for confirming heparan sulfate-mutant CHO-cells identities; Thomas Dierks (University of Bielefeld, Germany) for Sulf-deficient cells and tissues; Ruey-Bing Yang (Academia Sinica, Taiwan) for human Scube2; and Eva Korpos, Jeannine Wegner and Sabine Kupich for supporting this project.

Competing interests

The authors declare no competing or financial interests.

Author contributions

C.O., U.P., S.E., S.O., H.J., R.L., and K.G. performed experiments; C.O., U.P., R.D. and K.G. perceived, designed and interpreted experiments; C.O. and K.G. wrote the paper.

Funding

This work was financed by Deutsche Forschungsgemeinschaft (DFG, German Research Council) [grant numbers SFB 492-B15, GRK1549/1]; and the IMF fund of the University of Münster Medical School and the Maria Möller Stiftung [grant number I-GR221408].

Supplementary material

Supplementary material available online at
http://jcs.biologists.org/lookup/suppl/doi:10.1242/jcs.170670/-/DC1

References

Amanai, K. and Jiang, J. (2001). Distinct roles of Central missing and Dispatched in sending the Hedgehog signal. *Development* **128**, 5119-5127.

Axelsson, J., Xu, D., Kang, B. N., Nussbacher, J. K., Handel, T. M., Ley, K., Sriramarao, P. and Esko, J. D. (2012). Inactivation of heparan sulfate 2-O-sulfotransferase accentuates neutrophil infiltration during acute inflammation in mice. *Blood* **120**, 1742-1751.

Ayers, K. L., Gallet, A., Staccini-Lavenant, L. and Thérond, P. P. (2010). The long-range activity of Hedgehog is regulated in the apical extracellular space by the glypican Dally and the hydrolase Notum. *Dev. Cell* **18**, 605-620.

Bai, X. and Esko, J. D. (1996). An animal cell mutant defective in heparan sulfate hexuronic acid 2-O-sulfation. *J. Biol. Chem.* **271**, 17711-17717.

Bellaiche, Y., The, I. and Perrimon, N. (1998). *Tout-velu* is a *Drosophila* homologue of the putative tumour suppressor EXT-1 and is needed for Hh diffusion. *Nature* **394**, 85-88.

Bennett, W. F. D., MacCallum, J. L., Hinner, M. J., Marrink, S. J. and Tieleman, D. P. (2009). Molecular view of cholesterol flip-flop and chemical potential in different membrane environments. *J. Am. Chem. Soc.* **131**, 12714-12720.

Bilioni, A., Sánchez-Hernández, D., Callejo, A., Gradilla, A.-C., Ibáñez, C., Mollica, E., Carmen Rodríguez-Navas, M., Simon, E. and Guerrero, I. (2013). Balancing Hedgehog, a retention and release equilibrium given by Dally, Ihog, Boi and shifted/DmWif. *Dev. Biol.* **376**, 198-212.

Bornemann, D. J., Duncan, J. E., Staatz, W., Selleck, S. and Warrior, R. (2004). Abrogation of heparan sulfate synthesis in Drosophila disrupts the Wingless, Hedgehog and Decapentaplegic signaling pathways. *Development* **131**, 1927-1938.

Bumcrot, D. A., Takada, R. and McMahon, A. P. (1995). Proteolytic processing yields two secreted forms of sonic hedgehog. *Mol. Cell Biol.* **15**, 2294-2303.

Butler, G. S., Butler, M. J., Atkinson, S. J., Will, H., Tamura, T., Schade van Westrum, S., Crabbe, T., Clements, J., d'Ortho, M.-P. and Murphy, G. (1998). The TIMP2 membrane type 1 metalloproteinase "receptor" regulates the concentration and efficient activation of progelatinase A: a kinetic study. *J. Biol. Chem.* **273**, 871-880.

Capurro, M. I., Xu, P., Shi, W., Li, F., Jia, A. and Filmus, J. (2008). Glypican-3 inhibits Hedgehog signaling during development by competing with patched for Hedgehog binding. *Dev. Cell* **14**, 700-711.

Cardin, A. D. and Weintraub, H. J. (1989). Molecular modeling of protein-glycosaminoglycan interactions. *Arterioscler. Thromb. Vasc. Biol.* **9**, 21-32.

Carlsson, P., Presto, J., Spillmann, D., Lindahl, U. and Kjellen, L. (2008). Heparin/heparan sulfate biosynthesis: processive formation of N-sulfated domains. *J. Biol. Chem.* **283**, 20008-20014.

Carrasco, H., Olivares, G. H., Faunes, F., Oliva, C. and Larraín, J. (2005). Heparan sulfate proteoglycans exert positive and negative effects in Shh activity. *J. Cell. Biochem.* **96**, 831-838.

Chamoun, Z., Mann, R. K., Nellen, D., von Kessler, D. P., Bellotto, M., Beachy, P. A. and Basler, K. (2001). Skinny hedgehog, an acyltransferase required for palmitoylation and activity of the hedgehog signal. *Science* **293**, 2080-2084.

Chan, J. A., Balasubramanian, S., Witt, R. M., Nazemi, K. J., Choi, Y., Pazyra-Murphy, M. F., Walsh, C. O., Thompson, M. and Segal, R. A. (2009). Proteoglycan interactions with Sonic Hedgehog specify mitogenic responses. *Nat. Neurosci.* **12**, 409-417.

Chang, S.-C., Mulloy, B., Magee, A. I. and Couchman, J. R. (2011). Two distinct sites in sonic hedgehog combine for heparan sulfate interactions and cell signaling functions. *J. Biol. Chem.* **286**, 44391-44402.

Chatterjee, S. and Mayor, S. (2001). The GPI-anchor and protein sorting. *Cell. Mol. Life Sci.* **58**, 1969-1987.

Creanga, A., Glenn, T. D., Mann, R. K., Saunders, A. M., Talbot, W. S. and Beachy, P. A. (2012). Scube/You activity mediates release of dually lipid-modified Hedgehog signal in soluble form. *Genes Dev.* **26**, 1312-1325.

Crozatier, M., Glise, B. and Vincent, A. (2004). Patterns in evolution: veins of the Drosophila wing. *Trends Genet.* **20**, 498-505.

Damhofer, H., Veenstra, V. L., Tol, J. A. M. G., van Laarhoven, H. W. M., Medema, J. P. and Bijlsma, M. F. (2015). Blocking Hedgehog release from pancreatic cancer cells increases paracrine signaling potency. *J. Cell Sci.* **128**, 129-139.

Dierker, T., Dreier, R., Petersen, A., Bordych, C. and Grobe, K. (2009). Heparan sulfate-modulated, metalloprotease-mediated sonic hedgehog release from producing cells. *J. Biol. Chem.* **284**, 8013-8022.

Dreier, R., Gunther, B. K., Mainz, T., Nemere, I. and Bruckner, P. (2008). Terminal differentiation of chick embryo chondrocytes requires shedding of a cell surface protein that binds 1,25-dihydroxyvitamin D3. *J. Biol. Chem.* **283**, 1104-1112.

Ericson, J., Morton, S., Kawakami, A., Roelink, H. and Jessell, T. M. (1996). Two critical periods of Sonic Hedgehog signaling required for the specification of motor neuron identity. *Cell* **87**, 661-673.

Esko, J. D. and Lindahl, U. (2001). Molecular diversity of heparan sulfate. *J. Clin. Invest.* **108**, 169-173.

Esko, J. D. and Selleck, S. B. (2002). Order out of chaos: assembly of ligand binding sites in heparan sulfate. *Annu. Rev. Biochem.* **71**, 435-471.

Etheridge, L. A., Crawford, T. Q., Zhang, S. and Roelink, H. (2010). Evidence for a role of vertebrate Disp1 in long-range Shh signaling. *Development* **137**, 133-140.

Farshi, P., Ohlig, S., Pickhinke, U., Hoing, S., Jochmann, K., Lawrence, R., Dreier, R., Dierker, T. and Grobe, K. (2011). Dual roles of the cardin-weintraub motif in multimeric sonic hedgehog. *J. Biol. Chem.* **286**, 23608-23619.

Gallet, A., Staccini-Lavenant, L. and Thérond, P. P. (2008). Cellular trafficking of the glypican Dally-like is required for full-strength Hedgehog signaling and wingless transcytosis. *Dev. Cell* **14**, 712-725.

Gao, X. and Hannoush, R. N. (2014). Method for cellular imaging of palmitoylated proteins with clickable probes and proximity ligation applied to Hedgehog, tubulin, and Ras. *J. Am. Chem. Soc.* **136**, 4544-4550.

Grobe, K., Inatani, M., Pallerla, S. R., Castagnola, J., Yamaguchi, Y. and Esko, J. D. (2005). Cerebral hypoplasia and craniofacial defects in mice lacking heparan sulfate Ndst1 gene function. *Development* **132**, 3777-3786.

Han, C., Belenkaya, T. Y., Khodoun, M., Tauchi, M. and Lin, X. (2004a). Distinct and collaborative roles of Drosophila EXT family proteins in morphogen signalling and gradient formation. *Development* **131**, 1563-1575.
Han, C., Belenkaya, T. Y., Wang, B. and Lin, X. (2004b). Drosophila glypicans control the cell-to-cell movement of Hedgehog by a dynamin-independent process. *Development* **131**, 601-611.
Hardy, R. Y. and Resh, M. D. (2012). Identification of N-terminal residues of sonic hedgehog important for palmitoylation by hedgehog acyltransferase. *J. Biol. Chem.* **287**, 42881-42889.
Hartl, T. A. and Scott, M. P. (2014). Wing tips: the wing disc as a platform for studying Hedgehog signaling. *Methods* **68**, 199-206.
Iba, K., Albrechtsen, R., Gilpin, B., Fröhlich, C., Loechel, F., Zolkiewska, A., Ishiguro, K., Kojima, T., Liu, W., Langford, J. K. et al. (2000). The cysteine-rich domain of human ADAM 12 supports cell adhesion through syndecans and triggers signaling events that lead to beta1 integrin-dependent cell spreading. *J. Cell Biol.* **149**, 1143-1156.
Jacob, L. and Lum, L. (2007). Deconstructing the hedgehog pathway in development and disease. *Science* **318**, 66-68.
Jakobs, P., Exner, S., Schurmann, S., Pickhinke, U., Bandari, S., Ortmann, C., Kupich, S., Schulz, P., Hansen, U., Seidler, D. G. et al. (2014). Scube2 enhances proteolytic Shh processing from the surface of Shh-producing cells. *J. Cell Sci.* **127**, 1726-1737.
Khare, N. and Baumgartner, S. (2000). Dally-like protein, a new *Drosophila* glypican with expression overlapping with *wingless*. *Mech. Dev.* **99**, 199-202.
Kheradmand, F. and Werb, Z. (2002). Shedding light on sheddases: role in growth and development. *BioEssays* **24**, 8-12.
Konitsiotis, A. D., Chang, S.-C., Jovanović, B., Ciepla, P., Masumoto, N., Palmer, C. P., Tate, E. W., Couchman, J. R. and Magee, A. I. (2014). Attenuation of hedgehog acyltransferase-catalyzed sonic Hedgehog palmitoylation causes reduced signaling, proliferation and invasiveness of human carcinoma cells. *PLoS ONE* **9**, e89899.
Koo, B.-H., Han, J. H., Yeom, Y. I. and Kim, D.-S. (2010). Thrombin-dependent MMP-2 activity is regulated by heparan sulfate. *J. Biol. Chem.* **285**, 41270-41279.
Kusche-Gullberg, M., Nybakken, K., Perrimon, N. and Lindahl, U. (2012). Drosophila heparan sulfate, a novel design. *J. Biol. Chem.* **287**, 21950-21956.
Lamanna, W. C., Baldwin, R. J., Padva, M., Kalus, I., ten Dam, G., van Kuppevelt, T. H., Gallagher, J. T., von Figura, K., Dierks, T. and Merry, C. L. R. (2006). Heparan sulfate 6-O-endosulfatases: discrete in vivo activities and functional co-operativity. *Biochem. J.* **400**, 63-73.
Lawrence, R., Olson, S. K., Steele, R. E., Wang, L., Warrior, R., Cummings, R. D. and Esko, J. D. (2008). Evolutionary differences in glycosaminoglycan fine structure detected by quantitative glycan reductive isotope labeling. *J. Biol. Chem.* **283**, 33674-33684.
Lee, J. D. and Treisman, J. E. (2001). Sightless has homology to transmembrane acyltransferases and is required to generate active Hedgehog protein. *Curr. Biol.* **11**, 1147-1152.
Lee, J. J., Ekker, S. C., von Kessler, D. P., Porter, J. A., Sun, B. I. and Beachy, P. A. (1994). Autoproteolysis in hedgehog protein biogenesis. *Science* **266**, 1528-1537.
Lee, J. D., Kraus, P., Gaiano, N., Nery, S., Kohtz, J., Fishell, G., Loomis, C. A. and Treisman, J. E. (2001). An acylatable residue of Hedgehog is differentially required in Drosophila and mouse limb development. *Dev. Biol.* **233**, 122-136.
Li, F., Shi, W., Capurro, M. and Filmus, J. (2011). Glypican-5 stimulates rhabdomyosarcoma cell proliferation by activating Hedgehog signaling. *J. Cell Biol.* **192**, 691-704.
Lidholt, K., Weinke, J. L., Kiser, C. S., Lugemwa, F. N., Bame, K. J., Cheifetz, S., Massagué, J., Lindahl, U. and Esko, J. D. (1992). A single mutation affects both N-acetylglucosaminyltransferase and glucuronosyltransferase activities in a Chinese hamster ovary cell mutant defective in heparan sulfate biosynthesis. *Proc. Natl. Acad. Sci. USA* **89**, 2267-2271.
Lindahl, U., Kusche-Gullberg, M. and Kjellén, L. (1998). Regulated diversity of heparan sulfate. *J. Biol. Chem.* **273**, 24979-24982.
Liu, X.-Q. (2000). Protein-splicing intein: genetic mobility, origin, and evolution. *Annu. Rev. Genet.* **34**, 61-76.
Marti, E., Bumcrot, D. A., Takada, R. and McMahon, A. P. (1995). Requirement of 19K form of Sonic hedgehog for induction of distinct ventral cell types in CNS explants. *Nature* **375**, 322-325.
Mayor, S. and Riezman, H. (2004). Sorting GPI-anchored proteins. *Nat. Rev. Mol. Cell Biol.* **5**, 110-120.
Micchelli, C. A., The, I., Selva, E., Mogila, V. and Perrimon, N. (2002). Rasp, a putative transmembrane acyltransferase, is required for Hedgehog signaling. *Development* **129**, 843-851.
Mullor, J. L., Calleja, M., Capdevila, J. and Guerrero, I. (1997). Hedgehog activity, independent of decapentaplegic, participates in wing disc patterning. *Development* **124**, 1227-1237.
Murai, T., Maruyama, Y., Mio, K., Nishiyama, H., Suga, M. and Sato, C. (2011). Low cholesterol triggers membrane microdomain-dependent CD44 shedding and suppresses tumor cell migration. *J. Biol. Chem.* **286**, 1999-2007.
Nakamura, T., Aikawa, T., Iwamoto-Enomoto, M., Iwamoto, M., Higuchi, Y., Maurizio, P., Kinto, N., Yamaguchi, A., Noji, S., Kurisu, K. et al. (1997). Induction of osteogenic differentiation by hedgehog proteins. *Biochem. Biophys. Res. Commun.* **237**, 465-469.
Nakato, H., Futch, T. A. and Selleck, S. B. (1995). The *division abnormally delayed (dally)* gene: a putative integral membrane proteoglycan required for cell division patterning during postembryonic development of the nervous system in *Drosophila*. *Development* **121**, 3687-3702.
Ohlig, S., Farshi, P., Pickhinke, U., van den Boom, J., Höing, S., Jakuschev, S., Hoffmann, D., Dreier, R., Schöler, H. R., Dierker, T. et al. (2011). Sonic hedgehog shedding results in functional activation of the solubilized protein. *Dev. Cell* **20**, 764-774.
Ohlig, S., Pickhinke, U., Sirko, S., Bandari, S., Hoffmann, D., Dreier, R., Farshi, P., Gotz, M. and Grobe, K. (2012). An emerging role of sonic hedgehog shedding as a modulator of heparan sulfate interactions. *J. Biol. Chem.* **287**, 43708-43719.
Oustah, A. A., Danesin, C., Khouri-Farah, N., Farreny, M.-A., Escalas, N., Cochard, P., Glise, B. and Soula, C. (2014). Dynamics of Sonic hedgehog signaling in the ventral spinal cord are controlled by intrinsic changes in source cells requiring Sulfatase 1. *Development* **141**, 1392-1403.
Pallerla, S. R., Pan, Y., Zhang, X., Esko, J. D. and Grobe, K. (2007). Heparan sulfate Ndst1 gene function variably regulates multiple signaling pathways during mouse development. *Dev. Dyn.* **236**, 556-563.
Palm, W., Swierczynska, M. M., Kumari, V., Ehrhart-Bornstein, M., Bornstein, S. R. and Eaton, S. (2013). Secretion and signaling activities of lipoprotein-associated hedgehog and non-sterol-modified hedgehog in flies and mammals. *PLoS Biol.* **11**, e1001505.
Panáková, D., Sprong, H., Marois, E., Thiele, C. and Eaton, S. (2005). Lipoprotein particles are required for Hedgehog and Wingless signalling. *Nature* **435**, 58-65.
Pepinsky, R. B., Zeng, C., Wen, D., Rayhorn, P., Baker, D. P., Williams, K. P., Bixler, S. A., Ambrose, C. M., Garber, E. A., Miatkowski, K. et al. (1998). Identification of a palmitic acid-modified form of human Sonic hedgehog. *J. Biol. Chem.* **273**, 14037-14045.
Porter, J. A., Ekker, S. C., Park, W.-J., von Kessler, D. P., Young, K. E., Chen, C.-H., Ma, Y., Woods, A. S., Cotter, R. J., Koonin, E. V. et al. (1996a). Hedgehog patterning activity: role of a lipophilic modification mediated by the carboxy-terminal autoprocessing domain. *Cell* **86**, 21-34.
Porter, J. A., Young, K. E. and Beachy, P. A. (1996b). Cholesterol modification of hedgehog signaling proteins in animal development. *Science* **274**, 255-259.
Purushothaman, A., Chen, L., Yang, Y. and Sanderson, R. D. (2008). Heparanase stimulation of protease expression implicates it as a master regulator of the aggressive tumor phenotype in myeloma. *J. Biol. Chem.* **283**, 32628-32636.
Resh, M. D. (2006). Palmitoylation of ligands, receptors, and intracellular signaling molecules. *Sci. STKE* **2006**, re14.
Rietveld, A., Neutz, S., Simons, K. and Eaton, S. (1999). Association of sterol- and glycosylphosphatidylinositol-linked proteins with Drosophila raft lipid microdomains. *J. Biol. Chem.* **274**, 12049-12054.
Rubin, J. B., Choi, Y. and Segal, R. A. (2002). Cerebellar proteoglycans regulate sonic hedgehog responses during development. *Development* **129**, 2223-2232.
Ryu, H.-Y., Lee, J., Yang, S., Park, H., Choi, S., Jung, K.-C., Lee, S.-T., Seong, J.-K., Han, I.-O. and Oh, E.-S. (2009). Syndecan-2 functions as a docking receptor for pro-matrix metalloproteinase-7 in human colon cancer cells. *J. Biol. Chem.* **284**, 35692-35701.
Saad, O. M., Ebel, H., Uchimura, K., Rosen, S. D., Bertozzi, C. R. and Leary, J. A. (2005). Compositional profiling of heparin/heparan sulfate using mass spectrometry: assay for specificity of a novel extracellular human endosulfatase. *Glycobiology* **15**, 818-826.
Sorensen, H. P., Vives, R. R., Manetopoulos, C., Albrechtsen, R., Lydolph, M. C., Jacobsen, J., Couchman, J. R. and Wewer, U. M. (2008). Heparan sulfate regulates ADAM12 through a molecular switch mechanism. *J. Biol. Chem.* **283**, 31920-31932.
Strigini, M. and Cohen, S. M. (1997). A Hedgehog activity gradient contributes to AP axial patterning of the Drosophila wing. *Development* **124**, 4697-4705.
Tabata, T. and Kornberg, T. B. (1994). Hedgehog is a signaling protein with a key role in patterning Drosophila imaginal discs. *Cell* **76**, 89-102.
Takei, Y., Ozawa, Y., Sato, M., Watanabe, A. and Tabata, T. (2004). Three Drosophila EXT genes shape morphogen gradients through synthesis of heparan sulfate proteoglycans. *Development* **131**, 73-82.
Takeo, S., Akiyama, T., Firkus, C., Aigaki, T. and Nakato, H. (2005). Expression of a secreted form of Dally, a Drosophila glypican, induces overgrowth phenotype by affecting action range of Hedgehog. *Dev. Biol.* **284**, 204-218.
Tellier, E., Canault, M., Rebsomen, L., Bonardo, B., Juhan-Vague, I., Nalbone, G. and Peiretti, F. (2006). The shedding activity of ADAM17 is sequestered in lipid rafts. *Exp. Cell Res.* **312**, 3969-3980.
The, I., Bellaiche, Y. and Perrimon, N. (1999). Hedgehog movement is regulated through *tout velu*–dependent synthesis of a heparan sulfate proteoglycan. *Mol. Cell* **4**, 633-639.
Theunissen, J.-W. and de Sauvage, F. J. (2009). Paracrine Hedgehog signaling in cancer. *Cancer Res.* **69**, 6007-6010.
Tian, H., Callahan, C. A., DuPree, K. J., Darbonne, W. C., Ahn, C. P., Scales, S. J. and de Sauvage, F. J. (2009). Hedgehog signaling is restricted to the stromal

compartment during pancreatic carcinogenesis. *Proc. Natl. Acad. Sci. USA* **106**, 4254-4259.

Toyoda, H., Kinoshita-Toyoda, A., Fox, B. and Selleck, S. B. (2000). Structural analysis of glycosaminoglycans in animals bearing mutations in sugarless, sulfateless, and tout-velu: drosophila homologues of vertebrate genes encoding glycosaminoglycan biosynthetic enzymes. *J. Biol. Chem.* **275**, 21856-21861.

Tukachinsky, H., Kuzmickas, R. P., Jao, C. Y., Liu, J. and Salic, A. (2012). Dispatched and scube mediate the efficient secretion of the cholesterol-modified hedgehog ligand. *Cell Rep.* **2**, 308-320.

Vyas, N., Goswami, D., Manonmani, A., Sharma, P., Ranganath, H. A., VijayRaghavan, K., Shashidhara, L. S., Sowdhamini, R. and Mayor, S. (2008). Nanoscale organization of hedgehog is essential for long-range signaling. *Cell* **133**, 1214-1227.

Williams, E. H., Pappano, W. N., Saunders, A. M., Kim, M.-S., Leahy, D. J. and Beachy, P. A. (2010). Dally-like core protein and its mammalian homologues mediate stimulatory and inhibitory effects on Hedgehog signal response. *Proc. Natl. Acad. Sci. USA* **107**, 5869-5874.

Wilson, C. W. and Chuang, P.-T. (2006). New “hogs” in Hedgehog transport and signal reception. *Cell* **125**, 435-438.

Wojcinski, A., Nakato, H., Soula, C. and Glise, B. (2011). DSulfatase-1 fine-tunes Hedgehog patterning activity through a novel regulatory feedback loop. *Dev. Biol.* **358**, 168-180.

Xu, D. and Esko, J. D. (2014). Demystifying heparan sulfate–protein interactions. *Annu. Rev. Biochem.* **83**, 129-157.

Yang, P., Baker, K. A. and Hagg, T. (2006). The ADAMs family: coordinators of nervous system development, plasticity and repair. *Prog. Neurobiol.* **79**, 73-94.

Yasuda, T., Mundy, C., Kinumatsu, T., Shibukawa, Y., Shibutani, T., Grobe, K., Minugh-Purvis, N., Pacifici, M. and Koyama, E. (2010). Sulfotransferase Ndst1 is needed for mandibular and TMJ development. *J. Dent. Res.* **89**, 1111-1116.

Yauch, R. L., Gould, S. E., Scales, S. J., Tang, T., Tian, H., Ahn, C. P., Marshall, D., Fu, L., Januario, T., Kallop, D. et al. (2008). A paracrine requirement for hedgehog signalling in cancer. *Nature* **455**, 406-410.

Zeng, X., Goetz, J. A., Suber, L. M., Scott, W. J., Jr, Schreiner, C. M. and Robbins, D. J. (2001). A freely diffusible form of Sonic hedgehog mediates long-range signalling. *Nature* **411**, 716-720.

Zhang, F., McLellan, J. S., Ayala, A. M., Leahy, D. J. and Linhardt, R. J. (2007). Kinetic and structural studies on interactions between heparin or heparan sulfate and proteins of the hedgehog signaling pathway. *Biochemistry* **46**, 3933-3941.

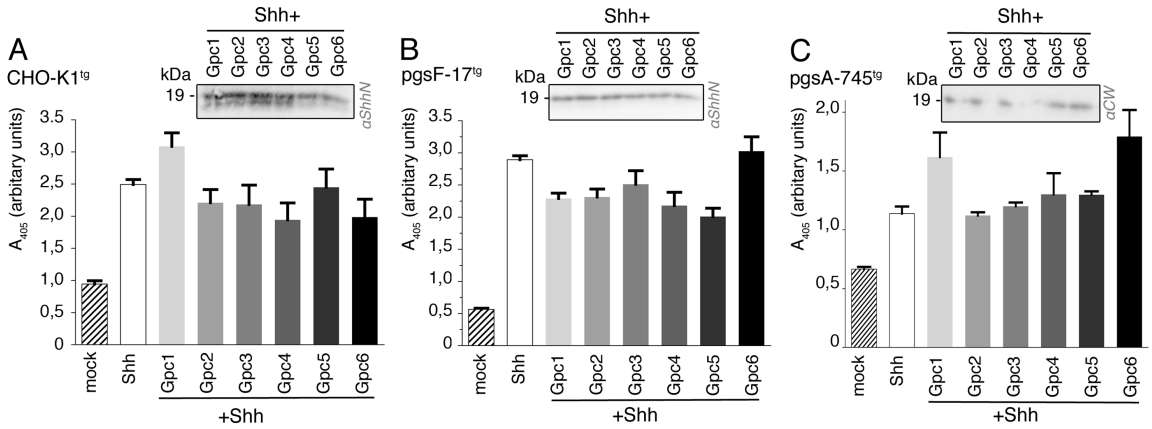

Fig. S1: A-C) Shh release and biofunction in Hhat-transfected CHO-K1^{tg}, pgsF-17^{tg} and pgsA-745^{tg} cells. Gpcs 1-6 and Shh were co-expressed in CHO cells from bicistronic mRNAs. released into serum free media for 24h and the soluble protein amounts were quantified. Supernatants of Gpc/Shh expressing CHO cells, or control media conditioned with (Shh) or without Shh (mock) were added to C3H10T1/2 osteoblast precursor cells, and Hh-dependent cell differentiation was determined. Gpc core proteins do not significantly affect Shh bioactivity in CHO-K1^{tg} cells (with the exception of Gpc1)(A), CHO pgsF-17^{tg} (with the exception of Gpc6)(B) and CHO pgsA-745^{tg} cells (with the exception of Gpc1 and Gpc6)(C). CHO K1^{tg} cells: Shh alone (control): 2.5±0.08 arbitary units (au) (n=9), Gpc1/Shh 3.1±0.2 au, p=0.01, n=8, Gpc2/Shh 2.2±0.2 au p=0.21, n=9, Gpc3/Shh 2.18±0.3 au, p=0.33, n=9, Gpc4/Shh 1.9±0.26 au, p-value 0.06, n=9, Gpc5/Shh 2.4±0.28 au, p=0.89, n=9, Gpc6/Shh 1.987±0.2779 au, p-value 0.0989, n=9. For pgsF-17^{tg} cells: Shh 2.893±0.06 au, n=9, Gpc1/Shh 2.29±0.08 au, p=0.0001, n=9, Gpc2/Shh 2.3±0.12 au, p=0.0007, n=9, Gpc3/Shh 2.5±0.21 au, p=0.1, n=9, Gpc4/Shh 2.18±0.21 au, p=0.0044, n=9, Gpc5/Shh 2±0.13 au, p=0.0001, n=9, Gpc6/Shh 3±0.22 au, p=0.57, n=9 and for pgsA-745^{tg} cells: Shh 1.14±0.06 au, n=9, Gpc1/Shh 1.62±0.2 au, p=0.0416, n=9, Gpc2/Shh 1.1±0.03 au, p=0.8, n=9, Gpc3/Shh 1.2±0.03 au, p=0.37, n=9, Gpc4/Shh 1.3±0.18 au, p=0.4, n=9, Gpc5/Shh 1.3±0.09 au, p=0.03, n=9, Gpc6/Shh 1.8±0.22 au, p=0.01, n=9.

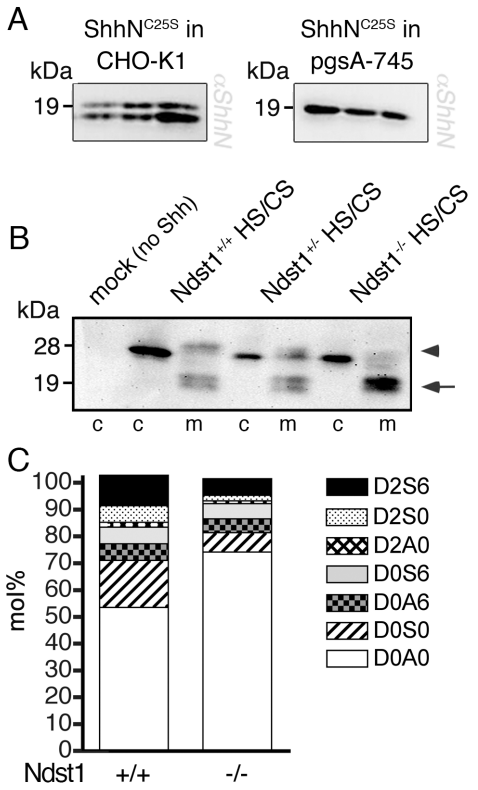

Fig. S2: A) Unlipidated $ShhN^{C25S}$ is secreted from CHO-$K1^{tg}$ and pgs-$A745^{tg}$ cells into the supernatant, but only the CHO-$K1^{tg}$ secreted material is N-terminally processed. This demonstrates that HS-expression is a critical determinant of Shh processing. Processed proteins show increased electrophoretic mobility. **B)** HS was isolated from E18 C57/Bl6 mice, Ndst1 heterozygous or homozygous mutant embryos, and analyzed as described before. Although the processing cellular material was potentiated by all HS isolates, only HS isolated from Ndst1 mutant embryos stabilized the product, resembling results obtained by pooled EHS obtained from E12.5-E18 mouse embryos (Fig. 6). In contrast, HS derived from wildtype littermate controls resembled CHS-facilitated Shh processing. This demonstrates that HS, not the CS fraction also present in the isolates, potentiates Hh processing an agreement with glypicans being HS-proteoglycans, not CS proteoglycans. **C)** HS was isolated and samples digested with heparin lyases. The resulting disaccharides were analyzed by quantitative LC/MS. Values denote the mean % of total disaccharide. The abbreviations used denote the following disaccharides: D0A0 (ΔUA1,4GlcNAc), D0S0 (ΔUA1,4GlcNS), D0A6 (ΔUA1,4GlcNAc-6S), D0S6 (ΔUA1,4GlcNS-6S), D2A0 (ΔUA2S1,4GlcNAc), D2S0 (ΔUA2S1,4GlcNS) and D2S6 (ΔUA2S1,4GlcNS-6S). Overall HS sulfation of the $Ndst1^{-/-}$ material was 1/3 reduced if compared to HS isolated from wild-type or heterozygous littermate controls.

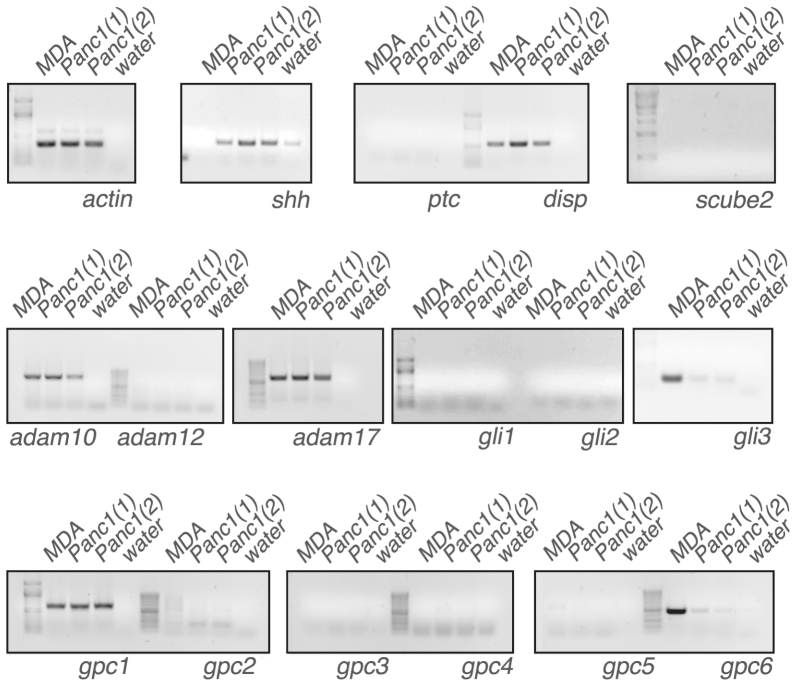

Fig. S3: PANC cells express genes required for Shh production and release, but not for Shh reception, as determined by semiquantitative RT-PCR. Assays were performed in duplicate, and MDA cells served as a control. We detected lack of scube2 and adam12 mRNA expression consistent with previous reports (Creanga et al., 2012; Damhofer et al., 2015; Tukachinsky et al., 2012).

References:

Creanga, A., Glenn, T. D., Mann, R. K., Saunders, A. M., Talbot, W. S. and Beachy, P. A. (2012). Scube/You activity mediates release of dually lipid-modified Hedgehog signal in soluble form. *Genes Dev* **26**, 1312-25.

Damhofer, H., Veenstra, V. L., Tol, J. A., van Laarhoven, H. W., Medema, J. P. and Bijlsma, M. F. (2015). Blocking Hedgehog release from pancreatic cancer cells increases paracrine signaling potency. *J Cell Sci* **128**, 129-139.

Tukachinsky, H., Kuzmickas, R. P., Jao, C. Y., Liu, J. and Salic, A. (2012). Dispatched and scube mediate the efficient secretion of the cholesterol-modified hedgehog ligand. *Cell Rep* **2**, 308-20.

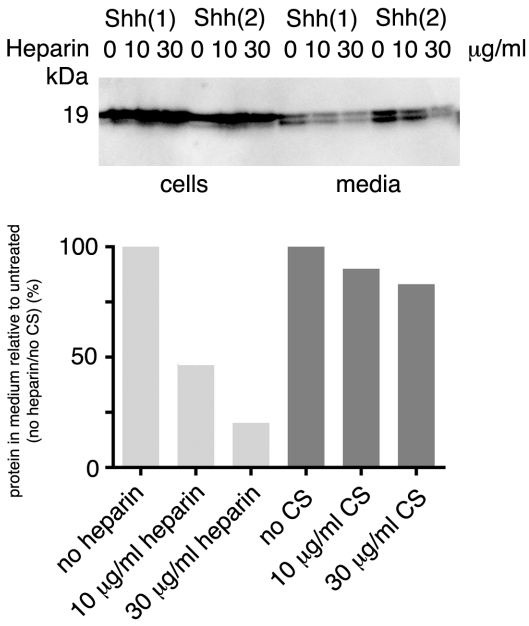

Fig. S4: Shh expression in the presence or absence of 0-30μg/ml heparin and chondroitin sulfate (CS). Heparin blocked Shh processing and release in concentration-dependent manner.